universe

IMPACT FACTOR 2.5

CITESCORE 4.3

Article

Stochastic Tunneling in de Sitter Spacetime

Taiga Miyachi, Jiro Soda and Junsei Tokuda

Special Issue
Cosmological Models of the Universe

Edited by
Prof. Dr. Panayiotis Stavrinos and Prof. Dr. Emmanuel N. Saridakis

MDPI

https://doi.org/10.3390/universe10070292

universe

MDPI

Article

Stochastic Tunneling in de Sitter Spacetime

Taiga Miyachi [1,*], Jiro Soda [1,2] and Junsei Tokuda [3]

[1] Department of Physics, Kobe University, Kobe 657-8501, Japan; jiro@phys.sci.kobe-u.ac.jp
[2] International Center for Quantum-Field Measurement Systems for Studies of the Universe and Particles (QUP), KEK, Tsukuba 305-0801, Japan
[3] Particle Theory and Cosmology Group, Center for Theoretical Physics of the Universe, Institute for Basic Science (IBS), Daejeon 34126, Republic of Korea; jtokuda@ibs.re.kr
* Correspondence: tmiyachi@stu.kobe-u.ac.jp

Abstract: Tunneling processes in de Sitter spacetime are studied by using the stochastic approach. We evaluate the Martin–Siggia–Rose–Janssen–de Dominicis (MSRJD) functional integral by using the saddle-point approximation to obtain the tunneling rate. The applicability conditions of this method are clarified using the Schwinger–Keldysh formalism. In the case of a shallow potential barrier, we reproduce the Hawking–Moss (HM) tunneling rate. Remarkably, in contrast to the HM picture, the configuration derived from the MSRJD functional integral satisfies physically natural boundary conditions. We also discuss the case of a steep potential barrier and find an interesting Coleman–de Luccia (CDL) bubblelike configuration. Since the starting point of our analysis is the Schwinger–Keldysh path integral, which can be formulated in a more generic setup and incorporates quantum effects, our formalism sheds light on further studies of tunneling phenomena from a real-time perspective.

Keywords: tunneling; stochastic approach; de Sitter spacetime; MSRJD functional integral

check for updates

Citation: Miyachi, T.; Soda, J.; Tokuda, J. Stochastic Tunneling in de Sitter Spacetime. *Universe* **2024**, *10*, 292. https://doi.org/10.3390/universe10070292

Academic Editors: Panayiotis Stavrinos and Emmanuel N. Saridakis

Received: 2 June 2024
Revised: 8 July 2024
Accepted: 10 July 2024
Published: 11 July 2024

1. Introduction

Tunneling is an important nonperturbative phenomenon in cosmology. Hence, it is crucial to understand tunneling processes in curved spacetime. In particular, tunneling in de Sitter spacetime is worth studying in detail. The reason is that the de Sitter spacetime is the simplest non-trivial curved spacetime. Moreover, the results obtained there can be applicable to tunneling phenomena during inflation. Since both Minkowski and de Sitter spacetime have the maximal symmetry, there exist a similarity. Indeed, the Euclidean instanton method for evaluating the tunneling rate in Minkowski spacetime [1,2] is applicable to tunneling processes in de Sitter spacetime [3]. However, the extension of the Euclidean method to the de Sitter spacetime has a difficulty in interpretation. In the case of the de Sitter spacetime, there are two saddle solutions: Coleman–De Luccia (CDL) [3] and Hawking–Moss (HM) instantons [4]. The latter instanton is a homogeneous solution. Therefore, it is not straightforward to interpret the tunneling rate as that for the tunneling process from a false vacuum to a true vacuum [5,6].

To circumvent the difficulty, a real-time formalism might be useful. In the case of the de Sitter spacetime in the flat chart, the stochastic formalism has been used for investigating time evolution of fluctuations during inflation [7,8]. In this formalism, Langevin equations describe the dynamics of long-wavelength modes. Stochastic noises stem from short-wavelength quantum modes. The stochastic formalism has also been used to analyze the tunneling processes in de Sitter spacetime [9–15]. However, most of the previous works treated only the HM transition by utilizing the Fokker–Plank (FP) equation for a homogeneous scalar field, which can be derived from the Langevin equation. Obviously, the HM transition cannot describe the bubble nucleation in contrast to CDL tunneling. To describe the bubble, we have to include the spatial gradient term, and the FP equation becomes a

functional differential equation instead of a partial differential equation. Hence, at first glance, it seems difficult to treat the CDL bubble by the stochastic approach. However, we make an observation that there exists a path integral representation to solutions of the FP equation. In condensed matter physics, it is called the Martin–Siggia–Rose–Janssen–de Dominicis (MSRJD) functional integral [16–19].

In this paper, we use the MSRJD path integral formula to study the tunneling processes on the fixed de Sitter background. The applicability conditions of this method are clarified based on the Schwinger–Keldysh formalism. We consider a potential $V(\phi)$ which has a local minimum at $\phi = \phi_{\rm false}$, a true minimum at $\phi_{\rm true}$, and a local maximum at $\phi_{\rm top}$ as shown in Figure 1. We use the saddle-point method and evaluate the tunneling rate by computing the action for the tunneling configurations [20]. We investigate both HM and CDL tunneling processes. In the case of a shallow potential barrier, the conventional HM tunneling rate is reproduced. Remarkably, the tunneling configuration in the MSRJD functional integral method has physically natural boundary conditions in contrast to the Euclidean method. We then clarify that the HM tunneling rate is the tunneling rate of a (roughly Hubble sized) coarse-grained patch transitioning from $\phi_{\rm false}$ to $\phi_{\rm top}$. In the case of a steep potential barrier, we find an interesting CDL bubblelike configuration which is obtained by solving the solution of a scalar field equation in Euclidean anti-de Sitter space even though we do not work in the imaginary time. Our results show how the bubble nucleation process could be described in the stochastic approach.

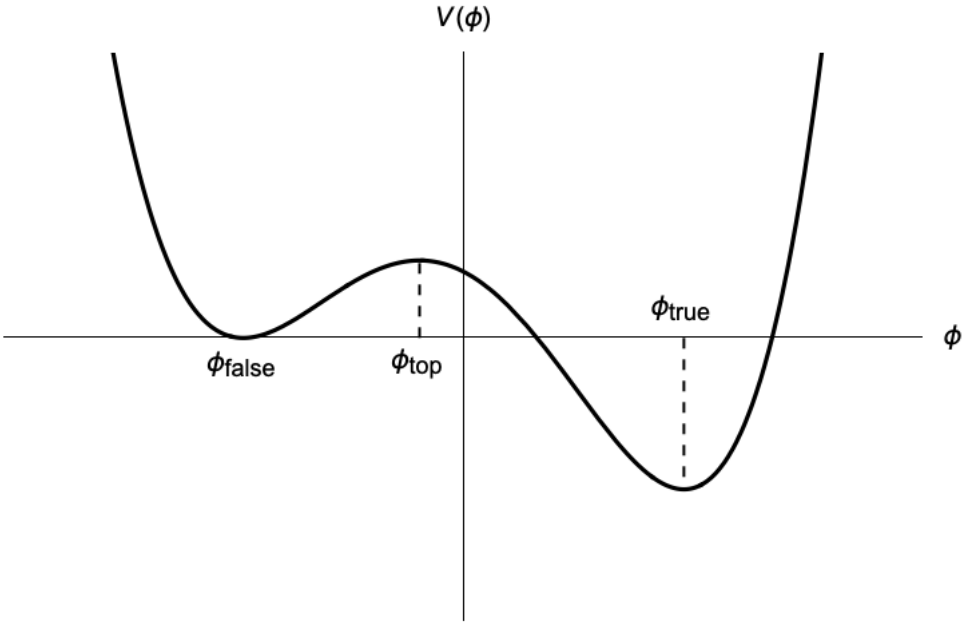

Figure 1. The schematic picture of the potential $V(\phi)$ which has a false vacuum at $\phi = \phi_{\rm false}$, true vacuum at $\phi = \phi_{\rm true}$ and the top of the potential at $\phi = \phi_{\rm top}$.

This paper is organized as follows. In Section 2, we present the setup and review the stochastic approach. In Section 3, the MSRJD functional integral is constructed from the Langevin equations. We also outline the derivation of the MSRJD functional integral starting from the Schwinger–Keldysh formalism. In Section 4, we apply the MSRJD functional integral to the case of the shallow potential barrier and study the HM tunneling process. In Section 5, we consider the case of the steep potential barrier and find the CDL bubblelike configuration. We derive the tunneling rate using the configuration and compare it with the one obtained in Section 4. We also compare our results with those in the Euclidean method. Section 6 is devoted to the conclusion. Some technical details are presented in appendices.

2. Stochastic Approach

In this section, we review the stochastic approach [7,8].

2.1. Setup

We consider a real scalar field ϕ in a (3 + 1)-dimensional de Sitter background. The background geometry is described by the metric

$$ds^2 = -dt^2 + a(t)^2 d\boldsymbol{x}^2 = a(\eta^2)(-d\eta^2 + d\boldsymbol{x}^2), \tag{1}$$

with the scale factor

$$a(t) = e^{Ht} = -\frac{1}{H\eta}, \tag{2}$$

where H is the Hubble constant. The action is given by

$$S = \int dt d^3x\, a^3 \left[\frac{1}{2}\dot{\phi}^2 - \frac{1}{2}a^{-2}(\nabla\phi)^2 - V(\phi)\right], \tag{3}$$

where a dot denotes a derivative with respect to t and $V(\phi)$ is a potential function. From this action, the canonical conjugate momentum Π is defined as $\Pi := a^3\dot{\phi}$ and the Hamilton's equations of motion are given by

$$\dot{\phi} = a^{-3}\Pi\,, \qquad \dot{\Pi} = a\nabla^2\phi - a^3 V'(\phi)\,. \tag{4}$$

2.2. Langevin Equation

First, we divide the quantum fields ϕ and Π into an infrared (IR) part and an ultraviolet (UV) part, respectively, as

$$\phi = \phi_{\rm IR} + \phi_{\rm UV}\,, \qquad \Pi = \Pi_{\rm IR} + \Pi_{\rm UV}\,. \tag{5}$$

The UV part is defined as

$$\begin{aligned}
\phi_{\rm UV} &:= \int \frac{d^3k}{(2\pi)^3}\theta(k - k_c(t))\left[a_{\boldsymbol{k}} u_{\boldsymbol{k}}(t) e^{i\boldsymbol{k}\cdot\boldsymbol{x}} + a^\dagger_{\boldsymbol{k}} u^*_{\boldsymbol{k}}(t) e^{-i\boldsymbol{k}\cdot\boldsymbol{x}}\right], \\
\Pi_{\rm UV} &:= \int \frac{d^3k}{(2\pi)^3}\theta(k - k_c(t)) a(t)^3 \left[a_{\boldsymbol{k}} \dot{u}_{\boldsymbol{k}}(t) e^{i\boldsymbol{k}\cdot\boldsymbol{x}} + a^\dagger_{\boldsymbol{k}} \dot{u}^*_{\boldsymbol{k}}(t) e^{-i\boldsymbol{k}\cdot\boldsymbol{x}}\right],
\end{aligned} \tag{6}$$

where $u_{\boldsymbol{k}}$ is a mode function that is specified later, and $a_{\boldsymbol{k}}$ and $a^\dagger_{\boldsymbol{k}}$ are annihilation and creation operators, respectively. Here, $\theta(k - k_c(t))$ is a step function, and $k_c(t)$ is the cut-off scale defined as

$$k_c(t) := \varepsilon a(t) H, \tag{7}$$

where ε is a constant. The value of ε is discussed later. Substituting Equation (6) into Hamilton's Equation (4), we obtain the following equations;

$$\dot{\phi}_{\rm IR} = a^{-3}\Pi_{\rm IR} + \xi^\phi\,, \qquad \dot{\Pi}_{\rm IR} = a\nabla^2\phi_{\rm IR} - a^3 V'(\phi_{\rm IR}) + \xi^\Pi\,, \tag{8}$$

where ξ^ϕ and ξ^Π are defined as

$$\begin{aligned}
\xi^\phi &:= \dot{k}_c(t) \int \frac{d^3k}{(2\pi)^3}\delta(k - k_c(t))\left[a_{\boldsymbol{k}} u_{\boldsymbol{k}}(t) e^{i\boldsymbol{k}\cdot\boldsymbol{x}} + a^\dagger_{\boldsymbol{k}} u^*_{\boldsymbol{k}}(t) e^{-i\boldsymbol{k}\cdot\boldsymbol{x}}\right], \\
\xi^\Pi &:= \dot{k}_c(t) \int \frac{d^3k}{(2\pi)^3}\delta(k - k_c(t))\left[a_{\boldsymbol{k}} a(t)^3 \dot{u}_{\boldsymbol{k}}(t) e^{i\boldsymbol{k}\cdot\boldsymbol{x}} + a^\dagger_{\boldsymbol{k}} a(t)^3 \dot{u}^*_{\boldsymbol{k}}(t) e^{-i\boldsymbol{k}\cdot\boldsymbol{x}}\right].
\end{aligned} \tag{9}$$

To derive Equations (8) and (9), we assumed that the time evolution of UV modes could be well approximated by the free theory that is defined around the false vacuum. The mode function $u_{\boldsymbol{k}}(t)$ introduced in (9) then satisfies the following equation

$$\ddot{u}_{\boldsymbol{k}} + 3H\dot{u}_{\boldsymbol{k}} + a^{-2}k^2 u_{\boldsymbol{k}} + V''(\phi_{\rm false})u_{\boldsymbol{k}} = 0. \tag{10}$$

From this equation, we see the mode function only depends on $k := |\boldsymbol{k}|$. Hence, we simply denote the mode function as u_k. Note that this mode function is used for UV modes $k > k_c(t)$.

Let us consider statistical properties of ξ^ϕ and ξ^Π. The annihilation and creation operators $a_{\boldsymbol{k}}$ and $a^\dagger_{\boldsymbol{k}}$ satisfy the following commutation relations:

$$[a_{\boldsymbol{k}}, a^\dagger_{\boldsymbol{k}'}] = (2\pi)^3\delta^{(3)}(\boldsymbol{k}-\boldsymbol{k}')\,, \qquad [a_{\boldsymbol{k}}, a_{\boldsymbol{k}'}] = [a^\dagger_{\boldsymbol{k}}, a^\dagger_{\boldsymbol{k}'}] = 0. \tag{11}$$

Defining the vacuum state $|0\rangle$ as

$$a_{\boldsymbol{k}}\,|0\rangle = 0, \quad \forall \boldsymbol{k}, \tag{12}$$

we can calculate the one-point and two-point correlation functions of ξ^ϕ and ξ^Π as

$$\begin{aligned}
&\langle 0|\xi^\alpha(t,\boldsymbol{x})|0\rangle = 0, \quad (\alpha,\beta = \phi,\Pi),\\
&\langle 0|\xi^\alpha(t,\boldsymbol{x})\xi^\beta(t',\boldsymbol{x}')|0\rangle = \frac{1}{2\pi^2}\dot{k}_c(t)k_c(t)^2\,\frac{\sin(k_c(t)r)}{k_c(t)r}g^{\alpha\beta}(t)\delta(t-t'),
\end{aligned} \tag{13}$$

where $r := |\boldsymbol{x}-\boldsymbol{x}'|$, and

$$\begin{cases}
g^{\phi\phi}(t) & := |u_{k_c}(t)|^2\\
g^{\Pi\Pi}(t) & := a(t)^6|\dot{u}_{k_c}(t)|^2\\
g^{\phi\Pi}(t) & = (g^{\Pi\phi})^* := a(t)^3 u_{k_c}(t)\dot{u}^*_{k_c}(t).
\end{cases} \tag{14}$$

Because of the Wick theorem, all higher correlation functions can be decomposed into two-point functions. In the stochastic approach, we replace the operator ξ^α by the real random field which has the following statistical properties

$$\begin{aligned}
&\langle \xi^\alpha(t,\boldsymbol{x})\rangle_\xi = 0, \quad (\alpha,\beta = \phi,\Pi),\\
&\langle \xi^\alpha(t,\boldsymbol{x})\xi^\beta(t',\boldsymbol{x}')\rangle_\xi = \frac{1}{2\pi^2}\dot{k}_c(t)k_c(t)^2\,\frac{\sin(k_c(t)r)}{k_c(t)r}{\rm Re}[g^{\alpha\beta}(t)]\delta(t-t'),
\end{aligned} \tag{15}$$

where $\langle\cdots\rangle_\xi$ represents an expectation value with the distribution function of ξ^α. With this prescription, Equation (8) can be interpreted as the Langevin equations with the noise ξ^α stemming from quantum fluctuations. Since ξ^α are now regarded as classical variables, we ignore the imaginary parts of $g^{\phi\Pi}$ and $g^{\Pi\phi}$ which come from non-commutativity. Accordingly, IR variables $\phi_{\rm IR}$ and $\Pi_{\rm IR}$ are also regarded as classical stochastic variables in this prescription. The validity of this classical approximation is discussed in the next section.

2.3. Bunch–Davies Vacuum

Now we define the vacuum state $|0\rangle$ by specifying the mode function u_k. Equation (10) is the equation for the mode $k > k_c$. Let us assume that we can ignore the term V'' in solving (10). This can be justified when $|V''|$ is sufficiently small to satisfy $\max\left[(k_c/a)^2, H^2\right] \gg |V''|$. Under this approximation, (10) can be solved as

$$u_k = (-k\eta)^{\frac{3}{2}}\left[C_1 H^{(1)}_{\frac{3}{2}}(-k\eta) + C_2 H^{(2)}_{\frac{3}{2}}(-k\eta)\right], \tag{16}$$

where C_1, C_2 are constants of integration, and $H_\nu^{(1)}(z)$, $H_\nu^{(2)}(z)$ are Hankel functions. We choose the Bunch–Davies vacuum, i.e., the vacuum that coincides with Minkowski's vacuum at past infinity ($\eta \to -\infty$) so that

$$u_k \to \frac{-H\eta}{\sqrt{2k}} e^{-ik\eta}, \quad (-k\eta \to \infty). \tag{17}$$

This determines C_1, C_2 as

$$C_1 = -\sqrt{\frac{\pi}{4k}}\frac{H}{k}, \qquad C_2 = 0\,. \tag{18}$$

Thus, we obtain the mode function

$$u_k = \frac{H\eta}{\sqrt{2k}}\left(\frac{1}{-ik\eta} - 1\right)e^{-ik\eta}. \tag{19}$$

To check (17), we used the following formulae

$$H^{(1)}_{\frac{3}{2}}(z) = \sqrt{\frac{2}{\pi z}}\left(\frac{1}{iz} - 1\right)e^{iz}\,, \qquad H^{(2)}_{\frac{3}{2}}(z) = \sqrt{\frac{2}{\pi z}}\left(\frac{1}{-iz} - 1\right)e^{-iz}. \tag{20}$$

Substituting (19) into (14) and using (7), we obtain

$$\begin{cases} g^{\phi\phi} & = \frac{H^2\eta^2}{2k_c}\left(\frac{1}{k_c^2\eta^2} + 1\right) = \frac{1}{2Ha^3}\left(\varepsilon^{-3} + \varepsilon^{-1}\right) \\ g^{\Pi\Pi} & = \frac{k_c}{2H^2\eta^2} = \frac{Ha^3}{2}\varepsilon \\ g^{\phi\Pi} & = g^{\Pi\phi *} = \frac{1}{2}\left(\frac{1}{k_c\eta} + i\right) = -\frac{1}{2}\varepsilon^{-1} + \frac{i}{2} \end{cases}. \tag{21}$$

From (8), we have to scale $g^{\alpha\beta}$ as $g^{\phi\phi} \to g^{\phi\phi}$, $g^{\Pi\Pi} \to g^{\Pi\Pi}/(H^2a^6)$ and $g^{\phi\Pi} \to g^{\phi\Pi}/(Ha^3)$ in order to compare these quantities. Then, $g^{\phi\phi}$ and $g^{\Pi\Pi}$ become dominant for the case $\varepsilon \ll 1$ and $\varepsilon \gg 1$, respectively.

2.4. Reduced Langevin Equation

Let us focus on physics at the super-horizon scales by taking $\varepsilon \ll 1$ and assume a shallow potential so that we can use the massless approximation to evaluate the noise correlations. In this setup, we can use (21), from which we find that $g^{\phi\phi}$ becomes dominant. We then ignore the noise for momentum ξ^Π. We also ignore the gradient term in (8) because we focus on the physics at super-horizon scales. Since the potential is assumed to be shallow, the time variation in $\phi_{\rm IR}(t)$ is then very small. Therefore, we may integrate the second equation of (8) as

$$\Pi_{\rm IR} \simeq -\frac{a^3}{3H}V'(\phi_{\rm IR}). \tag{22}$$

Substituting this relation into the first equation of (8), we obtain

$$\dot{\phi}_{\rm IR} = -\frac{V'(\phi_{\rm IR})}{3H} + \xi^\phi, \tag{23}$$

where the two-point correlation function of ξ^ϕ is given at the leading order by

$$\langle \xi^\phi(t,\boldsymbol{x})\xi^\phi(t',\boldsymbol{x}')\rangle_\xi = \frac{H^3}{4\pi^2}j_0(k_cr)\delta(t-t')\,, \quad j_0(k_cr) := \frac{\sin(k_cr)}{k_cr}\,. \tag{24}$$

Equation (23) is the Langevin equation with the noise correlation (24) derived in [8].

3. Path Integral Formalism for the Stochastic Approach

In this section, we introduce a path integral approach for the Langevin equation following [21]. From now on, we replace the IR field and its conjugate momentum as $(\phi_{\rm IR}, \Pi_{\rm IR}) \to (\phi_c, \Pi_c)$. As we see in Section 3.2, this notation corresponds to the Keldysh basis. In Section 3.2, we provide a first-principle derivation of the stochastic approach based on the Schwinger–Keldysh formalism following [22,23][1]. We briefly show the sketch of the derivation in the main text, and details of derivations are given in Appendix A.

3.1. MSRJD Functional Integral Representation

3.1.1. Zero-Plus-One-Dimensional Theories

Equation (23) can be regarded as the equation determining the position of a particle $\phi(t)$ with the white noise ξ^ϕ defined by Equation (24). For $k_c r \ll 1$, we have $\sin(k_c r)/(k_c r) \simeq 1$ as a good approximation. Let us discretize the field and noise as $\phi_c(t) \to \phi_i$, $\xi^\phi(t) \to \xi^\phi_i$, $(i \in \mathbf{Z})$. Then, Equation (23) reads

$$X_i := \phi_i - \phi_{i-1} + \Delta t \left(\frac{V'(\phi_i)}{3H} - \xi^\phi_i \right) = 0, \tag{25}$$

where Δt is the temporal discretization interval. Note that the discretization (25) is called Ito discretization[2]. Denoting a solution of (23) by $\phi_c[\xi]$, the expectation value of an observable $\langle \mathcal{O} \rangle_\xi$ can be formally expressed as

$$\langle \mathcal{O}[\phi_c(t)] \rangle_\xi = \int \mathcal{D}\phi_c \, \mathcal{O}[\phi_c] \, \langle \delta(\phi_c - \phi_c[\xi]) \rangle_\xi = \int \mathcal{D}\phi_c \, \mathcal{O}[\phi_c] \left\langle \left| \frac{\delta X}{\delta \phi_c} \right| \delta(X) \right\rangle_\xi . \tag{26}$$

where $\mathcal{D}\phi_c := \prod_i d\phi_i$ is the functional measure, $\delta(\phi_c - \phi_c[\xi]) := \prod_i \delta(\phi_i - \phi_i[\xi])$, and $|\delta X/\delta \phi_c|$ is the determinant of $\{\delta X_i/\delta \phi_j\}$. When we choose the above discretization (25), $\delta X/\delta \phi_c$ becomes a triangular matrix with a unit in the diagonal components, i.e., the functional determinant is unity. Thus, substituting (25) into (26), we obtain

$$\langle \mathcal{O}[\phi_c(t)] \rangle_\xi = \int \mathcal{D}\phi_c \, \mathcal{O}[\phi_c] \left\langle \prod_i \delta \left(\phi_i - \phi_{i-1} + \Delta t \left(\frac{V'(\phi_i)}{3H} - \xi^\phi_i \right) \right) \right\rangle_\xi . \tag{27}$$

Representing the delta functions in terms of a Fourier integral and taking the continuum limit, we obtain the following path integral representation

$$\langle \mathcal{O}[\phi_c(t)] \rangle_\xi = \int \mathcal{D}(\phi_c, \tilde{\phi}) \, \mathcal{O}[\phi_c] \left\langle \exp \left[i \int \mathrm{d}t \tilde{\phi} \left(\dot{\phi}_c + \frac{V'(\phi_c)}{3H} - \xi^\phi \right) \right] \right\rangle_\xi . \tag{28}$$

After averaging over the noise assuming Gaussian statistics, we obtain the Martin–Siggia–Rose–Janssen–de Dominicis (MSRJD) functional integral

$$\langle \mathcal{O}[\phi_c(t)] \rangle_\xi = \int \mathcal{D}(\phi_c, \tilde{\phi}) \, \mathcal{O}[\phi_c] \exp \left[\int \mathrm{d}t \left(i\tilde{\phi} \left(\dot{\phi}_c + \frac{V'(\phi_c)}{3H} \right) - \frac{H^3}{8\pi^2} \tilde{\phi}^2 \right) \right]. \tag{29}$$

Putting $\mathcal{O}[\phi_c] = \delta(\phi_c - \phi_c(t))$ and taking the boundary conditions $\phi_c(t') = \phi'_c$ and $\phi_c(t) = \phi_c$, we obtain the transition probability $p(\phi_c, t | \phi'_c, t')$

$$p(\phi_c, t | \phi'_c, t') = \int_{\phi_c(t') = \phi'_c}^{\phi_c(t) = \phi_c} \mathcal{D}(\phi_c, \tilde{\phi}) \, \exp \left[\int \mathrm{d}t \left(i\tilde{\phi} \left(\dot{\phi}_c + \frac{V'(\phi_c)}{3H} \right) - \frac{H^3}{8\pi^2} \tilde{\phi}^2 \right) \right]. \tag{30}$$

Finally, introducing new variables $\Pi_\Delta := i\tilde{\phi}$, we obtain the "phase space" path integral

$$p(\phi_c, t | \phi'_c, t') = \int_{\phi_c(t') = \phi'_c}^{\phi_c(t) = \phi_c} \mathcal{D}(\phi_c, \Pi_\Delta) \, \exp \left[\int \mathrm{d}t (\Pi_\Delta \dot{\phi}_c - H(\phi_c, \Pi_\Delta)) \right], \tag{31}$$

where we defined the Hamiltonian as

$$H(\phi_c, \Pi_\Delta) := -\frac{V'(\phi_c)}{3H}\Pi_\Delta - \frac{H^3}{8\pi^2}\Pi_\Delta^2 \,. \tag{32}$$

We emphasize that this is just a change of integration variable, not the Wick rotation. A set of saddle-point equations is defined as the Hamilton equations for the Hamiltonian defined above.

3.1.2. Three-Plus-One-Dimensional Theories

Let us consider the case of the full Langevin Equations (8), (13) and (21). When the space is discretized, (8) can be seen as the dynamics of many body particles. Thus, the procedure in the previous subsection can be utilized. Taking the continuum limit, we obtain the following expression which is analogous to (30),

$$\begin{aligned} p(\phi_c(\boldsymbol{x}), t|\phi_c'(\boldsymbol{x}), t') = \int_{\phi_c(t',\boldsymbol{x})=\phi_c'(\boldsymbol{x})}^{\phi_c(t,\boldsymbol{x})=\phi_c(\boldsymbol{x})} \mathcal{D}(\phi_c, \Pi_c, \phi_\Delta, \Pi_\Delta) \\ \times \exp\left[i \int \mathrm{d}^4x \Big(\Pi_\Delta \dot{\phi}_c - \phi_\Delta \dot{\Pi}_c - H(\phi_c, \Pi_c, \phi_\Delta, \Pi_\Delta) \Big) \right]. \end{aligned} \tag{33}$$

We define the Hamiltonian $H(\phi_c, \Pi_c, \phi_\Delta, \Pi_\Delta)$ as

$$\begin{aligned} H(\phi_c, \Pi_c, \phi_\Delta, \Pi_\Delta) =& \frac{\Pi_c \Pi_\Delta}{a^3} - (a\nabla^2\phi_c - a^3 V'(\phi_c))\phi_\Delta \\ & - \frac{i}{2}\sum_{\alpha,\beta} \int \mathrm{d}^4x' X_\alpha(x) G^{\alpha\beta}(x, x') X_\beta(x') \,, \end{aligned} \tag{34}$$

where the Greek indices $\alpha, \beta = (\phi, \Pi)$ label the Δ fields as $(X_\phi, X_\Pi) = (\Pi_\Delta, -\phi_\Delta)$, and $G^{\alpha\beta}$ denotes the correlations of noises:

$$G^{\alpha\beta}(x, x') := \langle \xi^\alpha(x) \xi^\beta(x') \rangle_\xi \,, \tag{35}$$

where the RHS is given in (15). We use the formula (33) in Sections 4.2 and 5. Note that we have not changed the integration variables as $(\phi_\Delta, \Pi_\Delta) \to (-i\phi_\Delta, -i\Pi_\Delta)$.

In Sections 4 and 5, we take the initial state and the final state to be the false vacuum and the field configurations after tunneling (true vacuum or bubble), respectively.

3.2. Transition Probability from the Schwinger–Keldysh Formalism

In the above prescription, we treat IR fields $(\phi_{\rm IR}, \Pi_{\rm IR})$ as classical stochastic variables. To quantify the validity of this approximation, we derive the stochastic approach from the first principles based on the Schwinger–Keldysh formalism. Note that we use the label "IR" for IR fields in this subsection following the notation adopted in Appendix A.

Suppose that the system is in the false vacuum $|\Psi_{\rm false}\rangle$ at the past infinity $t = -\infty$, and it evolves into a certain quantum state $|\{\phi^{\rm IR}(T, \boldsymbol{x})\}_{\boldsymbol{x}\in\mathcal{D}}\rangle$ at the final time $t = T$, where $|\{\phi^{\rm IR}(T, \boldsymbol{x})\}_{\boldsymbol{x}\in\mathcal{D}}\rangle$ is an eigenstate of an IR field $\hat{\phi}^{\rm IR}(\boldsymbol{x})$ at spatial points $\boldsymbol{x}$ in the domain $\mathcal{D}$ with an eigenvalue $\phi^{\rm IR}(T, \boldsymbol{x})$. Here, $\hat{\phi}^{\rm IR}(\boldsymbol{x})$ is an IR field in the Schrödinger picture[3]. The transition probability p for this process is given by

$$p(\{\phi^{\rm IR}(T, \boldsymbol{x})\}_{\boldsymbol{x}\in\mathcal{D}}) = \left| \langle \{\phi^{\rm IR}(T, \boldsymbol{x})\}_{\boldsymbol{x}\in\mathcal{D}} | \hat{U}(t, -\infty) | \Psi_{\rm false} \rangle \right|^2 , \tag{36}$$

where $\hat{U}(t, t')$ describes the unitary time evolution from t' to t. The RHS is the Fourier component of the generating functional $Z[J^{\rm IR}]$ for IR fields, and we have

$$p(\{\phi^{\rm IR}(T,\boldsymbol{x})\}_{\boldsymbol{x}\in\mathcal{D}}) = \prod_{\boldsymbol{x}\in\mathcal{D}}\int {\rm d}J^{\rm IR}(T,\boldsymbol{x}) Z[J^{\rm IR}(T)] e^{-iJ^{\rm IR}(T,\boldsymbol{x})\phi^{\rm IR}(T,\boldsymbol{x})}\Big|_{\{J^{\rm IR}(T,\boldsymbol{y})=0\}_{\boldsymbol{y}\notin\mathcal{D}}}, \tag{37}$$

where the generating functional $Z[J^{\rm IR}(T)]$ is defined by

$$Z[J^{\rm IR}(T)] := {\rm Tr}\left[\hat{U}(T,-\infty)\left|\Psi_{\rm false}\right\rangle\left\langle\Psi_{\rm false}\right|\hat{U}^{\dagger}(T,-\infty)\prod_{\boldsymbol{x}} e^{iJ^{\rm IR}(T,\boldsymbol{x})\phi^{\rm IR}(T,\boldsymbol{x})}\right]. \tag{38}$$

We can evaluate $Z[J^{\rm IR}(T)]$ nonperturbatively in the IR sector based on the method developed in [22,23]. Our strategy is that we integrate out UV sector $k > k_c(t)$ perturbatively in nonlinear couplings to obtain $Z[J^{\rm IR}(T)]$. This is analogous to tracing out environmental degrees of freedom to evaluate the reduced density matrix for the system under considerations. Each step we take can be summarized as follows:

1. First, we derive a path integral representation of $Z[J^{\rm IR}(T)]$. We then split the integration variables into UV fields and IR fields such that the integration contour of UV variables of ϕ is closed; see discussions around Equation (A4) for more details[4].
2. We perform the integration over UV variables and evaluate an IR effective action, the so-called Feynman–Vernon influence functional [25] perturbatively.
3. We substitute the obtained expression of $Z[J^{\rm IR}(T)]$ into (37), giving rise to the path integral expression for the transition probability p.

Technical details are shown in Appendix A. At step 2, we assume that the quantum state for nonzero modes is given by the Bunch–Davies vacuum state for a free field defined around the false vacuum, and that the exact zero mode provides a non-fluctuating classical background field configuration $\phi = \phi_{\rm false}$.

In this way, we can obtain the path integral expression for the probability p as

$$p(\{\phi^{\rm IR}(T,\boldsymbol{x})\}_{\boldsymbol{x}\in\mathcal{D}}) = \int \mathcal{D}(\phi_c^{\rm IR},\phi_\Delta^{\rm IR},\Pi_c^{\rm IR},\Pi_\Delta^{\rm IR})\, e^{i\mathcal{S}}\,\delta[\mathcal{C}_{\rm fin}]\delta[\mathcal{C}_{\rm ini}]\,. \tag{39}$$

Here, $\delta[\mathcal{C}_{\rm fin}]$ and $\delta[\mathcal{C}_{\rm ini}]$ fix the boundary conditions of the path integral at the final time and the initial time, respectively:

$$\delta[\mathcal{C}_{\rm fin}] := \prod_{\boldsymbol{x}\in\mathcal{D}}\delta(\phi_c^{\rm IR}(T,\boldsymbol{x}) - \phi^{\rm IR}(T,\boldsymbol{x}))\prod_{\boldsymbol{y}}\delta(\phi_\Delta^{\rm IR}(T,\boldsymbol{y}))\,, \tag{40a}$$

$$\delta[\mathcal{C}_{\rm ini}] := \prod_{\boldsymbol{x}}\delta\Big(\phi_c^{\rm IR}(-\infty,\boldsymbol{x}) - \phi_{\rm false}\Big)\delta\Big(\Pi_c^{\rm IR}(-\infty,\boldsymbol{x})\Big)\delta[\mathcal{C}_{\rm detail}]\,, \tag{40b}$$

where $\delta[\mathcal{C}_{\rm detail}]$ is not relevant for the main points here, and we define it in Appendix A. A term $\mathcal{S}$ may be understood as an IR effective action,

$$\mathcal{S} := \int {\rm d}^4x\left[\Pi_\Delta^{\rm IR}\dot{\phi}_c^{\rm IR} - \phi_\Delta^{\rm IR}\dot{\Pi}_c^{\rm IR} - H(\phi_c^{\rm IR},\Pi_c^{\rm IR},\phi_\Delta^{\rm IR},\Pi_\Delta^{\rm IR}) - \delta H\right], \tag{41a}$$

$$\delta H := a^3(t)\left[V(\phi_c^{\rm IR} + (\phi_\Delta^{\rm IR}/2)) - V(\phi_c^{\rm IR} - (\phi_\Delta^{\rm IR}/2)) - V'(\phi_c^{\rm IR})\phi_\Delta^{\rm IR}\right] + \delta H_{\rm higher}\,, \tag{41b}$$

where H is given in (34). $\delta H_{\rm higher}$ denotes the higher-order terms in the coupling constant. Note that Equation (39) allows us to understand the transition probability p in terms of the stochastic dynamics: this point is discussed in Appendix A.3.

Validity of Equation (33)

Now, we find that $\mathcal{S}$ coincides with the term in the exponent of (33) up to the term δH. Hence, (39) shows that the result (33) in the previous section can be justified from the first principles when the term δH is negligible. Suppose that the potential $V(\phi)$ is sufficiently flat in the regime of interest such that the perturbation theory works when integrating out UV

modes. In this case, we can systematically calculate $\delta H_{\rm higher}$ perturbatively, and we have $\delta H_{\rm higher} = 0$ at the leading order. We set $\delta H_{\rm higher} = 0$ in the present analysis. We should keep in mind however that the nonperturbative physics at UV scales $k > k_c(t) = \varepsilon a(t) H$ is lost by setting $\delta H_{\rm higher} = 0$. From this viewpoint, we should choose ε as large as possible.

Even after setting $\delta H_{\rm higher} = 0$, we have nonzero δH. In the classical approximation, we may regard the Δ-variables $(\phi_\Delta^{\rm IR}, \Pi_\Delta^{\rm IR})$ as tiny quantities and keep only the terms which are linear in the Δ-variables in $\mathcal{S}$, leading to $\delta H \simeq 0$. In the case $\varepsilon \ll 1$, this approximation would work thanks to the squeezing of quantum fluctuations at super-horizon scales. However, it is more subtle if we can set $\delta H = 0$ in the case $\varepsilon \gtrsim 1$. We revisit this issue in Section 5.

4. Hawking–Moss Tunneling

In this section, we discuss the Hawking–Moss (HM) tunneling from the perspective of the MSRJD functional integral. We calculate the tunneling rate defined by (31) and (33) in Sections 4.1 and 4.2, respectively.

Hereafter, for the numerical calculations, we consider the potential [26] in Figure 2;

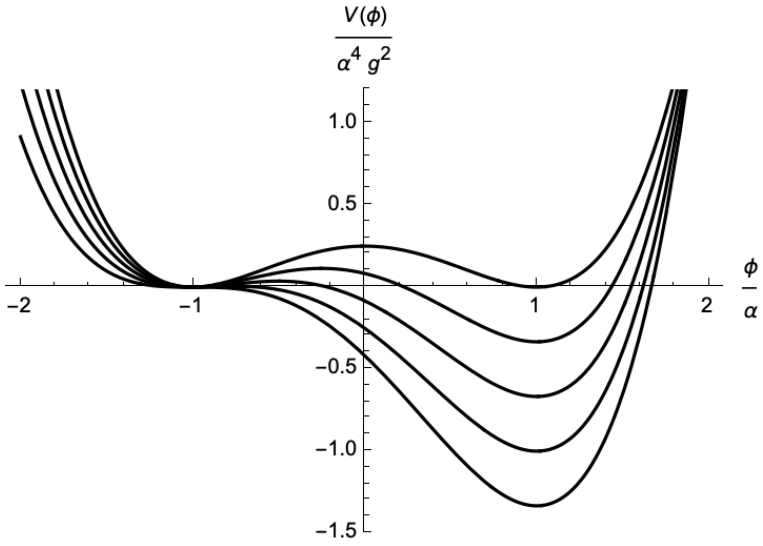

Figure 2. The potential of (42) for various β's. From top to bottom, the curves correspond to $\beta = 0, 0.25, 0.5, 0.75, 1$.

$$V(\phi) = \frac{g^2}{4}\left[(\phi^2 - \alpha^2)^2 + \frac{4\beta}{3}(\alpha\phi^3 - 3\alpha^3\phi - 2\alpha^4)\right], \tag{42}$$

for which the derivative with respect to ϕ is given by a simple form

$$V'(\phi) = g^2(\phi - \alpha)(\phi + \alpha)(\phi + \alpha\beta)\,. \tag{43}$$

For this potential, we have $\phi_{\rm false} = -\alpha$, $\phi_{\rm true} = \alpha$ and $\phi_{\rm top} = -\beta\alpha$. The dimensionless parameter β must be $0 < \beta < 1$, otherwise $\phi = -\alpha$ is not a false vacuum. The potential at each point takes the following values:

$$V(-\alpha) = 0\,, \quad V(\alpha) = -\frac{4\beta g^2\alpha^4}{3}\,, \quad V(-\beta\alpha) = \frac{g^2\alpha^4}{12}(1-\beta)^3(3+\beta)\,. \tag{44}$$

The height of potential barrier ΔV between the false vacuum and the true vacuum is

$$\Delta V := V(-\beta\alpha) - V(-\alpha) = \frac{g^2\alpha^4}{12}(1-\beta)^3(3+\beta)\,. \tag{45}$$

The mass of fluctuations around a given point ϕ is

$$V''(\phi) = \alpha^2 g^2 \left[3(\phi/\alpha)^2 + 2\beta(\phi/\alpha) - 1 \right]. \tag{46}$$

In our analysis, we work in the quantum field theory on the fixed de Sitter background. This assumption is valid when the condition $\max\left[|V(-\alpha)|, |V(-\beta\alpha)|, |V(\alpha)|\right] \ll 3M_{\rm pl}^2 H^2$ is satisfied. This is always satisfied when the following condition is imposed

$$H \ll \frac{3gM_{\rm pl}}{2}\left(\frac{H}{g\alpha}\right)^2 \approx 2.9 \times 10^{12}\,{\rm GeV}\left(\frac{g}{1.12\times 10^{-4}}\right)\left(\frac{\sqrt{140}}{g\alpha/H}\right)^2, \tag{47}$$

where we use $0 < \beta < 1$ and choose parameters $(g, g\alpha/H) = (1.12 \times 10^{-4}, \sqrt{140})$ as a benchmark point for later convenience. This shows that we can ignore the backreaction consistently with the weak coupling $g \ll 1$, provided that H is well below the Planck scale $M_{\rm pl} \approx 2.44 \times 10^{18}$ GeV. Note that under this condition, our discussion below is also applicable in the case of a quasi de Sitter background. However, it is non-trivial to generalize our analysis to the case when a non-negligible backreaction on H exists. This is because it is necessary to extend the first-principle derivation of the stochastic approach to account for the backreaction. This is in itself an interesting issue which we leave for future work.

4.1. The Case for the Reduced Langevin Equation

Let us start from the simpler formula (31). Hamilton's equations for the Hamiltonian $H(\phi_c, \Pi_\Delta)$ defined in (32) are given by

$$\begin{aligned} \dot{\phi}_c &= -\frac{V'(\phi_c)}{3H} - \frac{H^3}{4\pi^2}\Pi_\Delta \\ \dot{\Pi}_\Delta &= \frac{V''(\phi_c)}{3H}\Pi_\Delta. \end{aligned} \tag{48}$$

There exist many Hamiltonian flow lines in phase space (ϕ_c, Π_Δ) that represent the solution of Hamilton's equations as shown in Figure 3. Each flow line can be specified by the value of the Hamiltonian since it is conserved on the given flow line. In the Figure 3, there are two important flow lines corresponding to $H(\phi_c, \Pi_\Delta) = 0$. Since the Hamiltonian is the quadratic polynomial of Π_Δ, there are two Π_Δ satisfying $H(\phi_c, \Pi_\Delta) = 0$:

$$\Pi_\Delta = 0, -\frac{8\pi^2}{3H^4}V'. \tag{49}$$

In the case of $\Pi_\Delta = 0$, Equation (48) reduces to

$$\dot{\phi}_c = -\frac{V'(\phi_c)}{3H}. \tag{50}$$

Similarly, in the case of $\Pi_\Delta = -\frac{8\pi^2}{3H^4}V'(\phi_c)$, Equation (48) reduces to

$$\dot{\phi}_c = \frac{V'(\phi_c)}{3H}. \tag{51}$$

These two flow lines have three intersections which correspond to the false vacuum, the top of the potential hill and the true vacuum from left to right. On the flow line with $\Pi_\Delta = 0$, the false and true vacuums are stable and the top of the potential is unstable, while on the flow line with $\Pi_\Delta \neq 0$, the stability is reversed. The different signs of the potential forces account for the reverse of the stability at the intersections. We see that the tunneling configuration exists; starting from the false vacuum $(\phi_c, \Pi_\Delta) = (-\alpha, 0)$, going to the top of

the potential $(\phi_c, \Pi_\Delta) = (-\beta\alpha, 0)$ through the flow line with $\Pi_\Delta \neq 0$ and finally going to the true vacuum through the flow line with $\Pi_\Delta = 0$.

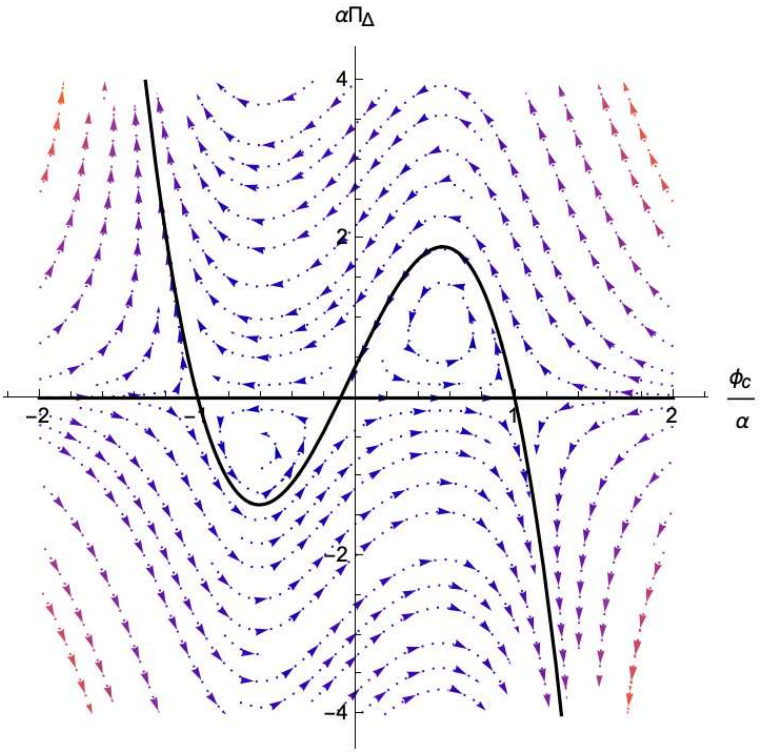

Figure 3. The Hamilton flow for (48) with $\alpha = H$, $g = 0.4$ and $\beta = 0.1$. The solid lines correspond to $H(\phi_c, \Pi_\Delta) = 0$. From left to right, the intersections of the solid lines correspond to the false vacuum, the top of the potential hill and the true vacuum.

We numerically solve the second equation with the initial conditions $\phi_c(t') = -\alpha$ and switch to the first equation when the field reaches the top of potential $\phi_c(t) = -\beta\alpha$. Thus, we obtain the tunneling configuration in Figure 4.

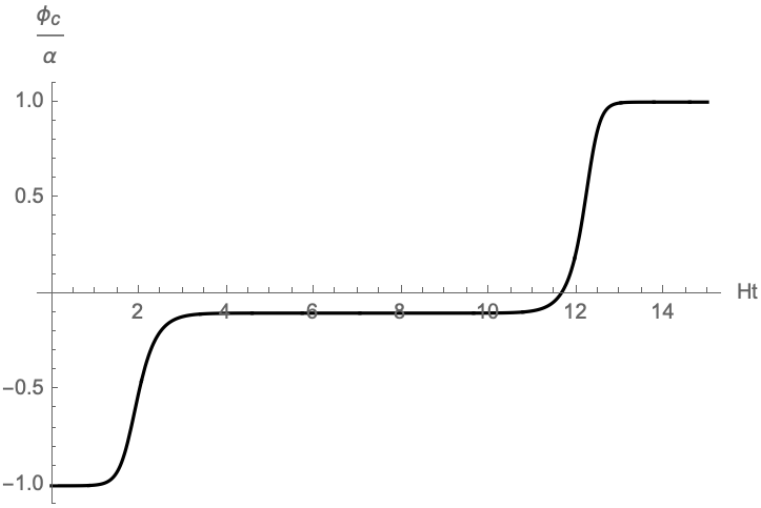

Figure 4. The tunneling configuration for the homogeneous fields is plotted for $\beta = 0.1$ and $\alpha g/H = \sqrt{10}$. We choose the initial condition as $\phi_c(10^{-15})/\alpha = -1 + 10^{-5}$ and solve the second equation of (50). When ϕ_c/α reach the top of potential $\phi_c/\alpha = -\beta$, we switch to the first equation of (50) with the initial condition $\phi_c/\alpha = -\beta + 10^{-5}$.

Now, we evaluate the transition probability (31) by substituting the above tunneling configurations. The action in (31) can be calculated without concrete solutions for ϕ_c;

$$I = \int_{t'}^{t} \mathrm{d}t[\Pi_\Delta \dot{\phi}_c - H(\phi_c, \Pi_\Delta)] = -\frac{8\pi^2}{3H^4}\int_{t'}^{t_*} \mathrm{d}t \dot{\phi}_c V'(\phi_c) = -\frac{8\pi^2}{3H^4}\Delta V, \tag{52}$$

where t_* is the time at which ϕ_c reaches the top of the potential, and ΔV is the difference of energy density between the top of the potential and the false vacuum. The trajectory from the top of the potential to the true vacuum does not contribute to the transition probability because $H(\phi_c, \Pi_\Delta) = 0$ and $\Pi_\Delta = 0$ on its trajectory. Thus, the transition probability of the tunneling can be evaluated as

$$p(\alpha, t|-\alpha, t') \sim \exp\left(-\frac{8\pi^2}{3H^4}\Delta V\right). \tag{53}$$

This shows a complete agreement with the result of the HM instanton on the fixed background [27].

Comments on this result are in order. It is pointed out in [27] that when the potential $V(\phi)$ has several degenerate local maxima, all of them yield the same tunneling action in the Euclidean method, despite differing distances from the false vacuum. In our formalism, however, a transition to a distant maximum is described by a saddle-point solution that passes through all the intermediate maxima, and the transition probability is given by the product of the factors on the RHS of (53) for each maximum. The aforementioned subtlety is absent in our formalism.

Since the analysis in Section 4.1 is based on (23) describing the stochastic dynamics of the IR field ϕ_c at a single spatial point, Equation (53) calculates the tunneling probability at a single spatial point, not on the whole universe[5]. Hence, physically speaking, (53) provides the tunneling probability of a coarse-grained patch with a physical radius $(\varepsilon H)^{-1}$. This point also becomes manifest in Section 4.2.

4.2. The Case for the Full Langevin Equation

Next, we evaluate the tunneling rate based on the formula (33). An advantage of (33) is that one can discuss various non-trivial dynamics in the whole universe covered by the flat chart in principle.

In the previous section, we focused on the dynamics at a single spatial point and found the HM tunneling process as a non-trivial solution of Hamilton's equations. In this section, we discuss the corresponding process in the global picture based on (33) by identifying a non-trivial configuration that satisfies Hamilton's equations in a good approximation. We then reproduce the result (52). We also estimate the characteristic time scale of the tunneling. In Section 4.2.1, we remark some technical complications that arise in the global picture.

We start with simplifying the expression (33). As discussed in Section 2, $G^{\phi\phi}$ becomes dominant, and the other terms can be neglected for $\varepsilon \ll 1$ in (34). Under this approximation, the exponent of the integrand of (33) is linear in ϕ_Δ. We can then perform the path integral $\int \mathcal{D}\phi_\Delta$ in (33), yielding the product of delta functions $\prod_{\boldsymbol{x}} \delta\left(\dot{\Pi}_c - a\nabla^2\phi_c + a^3 V'(\phi_c)\right)$. These delta functions give an equation of motion for Π_c and eliminate the path integral $\int \mathcal{D}\Pi_c$. We solve this equation as $\Pi_c \simeq -a^3 V'(\phi_c)/3H$, ignoring the spatial gradient and the time variation in ϕ_c. Furthermore, we change the integration variable as $\Pi_\Delta \to -i\Pi_\Delta$ in (33). Consequently, (33) reduces to

$$p(\phi_c(\boldsymbol{x}), t|\phi'_c(\boldsymbol{x}), t') \simeq \int_{\phi_c(t',\boldsymbol{x})=\phi'_c(\boldsymbol{x})}^{\phi_c(t,\boldsymbol{x})=\phi_c(\boldsymbol{x})} \mathcal{D}(\phi_c, \Pi_\Delta) \exp\left[\int \mathrm{d}^4x (\Pi_\Delta \dot{\phi}_c - H_{\mathrm{HM}}(\phi_c, \Pi_\Delta))\right], \tag{54}$$

where the Hamiltonian H_{HM} is defined as

$$H_{\rm HM}(\phi_c,\Pi_\Delta) := -\frac{1}{3H}V'(\phi_c)\Pi_\Delta - \frac{H^3}{8\pi^2}\Pi_\Delta\overline{\Pi}_\Delta\,, \tag{55}$$

and $\overline{\Pi}_\Delta$ is given by

$$\overline{\Pi}_\Delta(t,\boldsymbol{x}) := \int \mathrm{d}^3x'\, j_0\big(k_c(t)|\boldsymbol{x}-\boldsymbol{x}'|\big)\Pi_\Delta(t,\boldsymbol{x}') = \int \frac{\mathrm{d}^3k}{(2\pi)^3}\,\frac{4\pi^2}{H^3}\frac{H^2}{2k^3}\delta(t-t_k)\Pi_\Delta(t,\boldsymbol{k})e^{i\boldsymbol{k}\cdot\boldsymbol{x}}\,. \tag{56}$$

Here, we define t_k by the condition $k_c(t_k)=k$. Hamilton's equations are

$$\dot{\phi}_c = -\frac{1}{3H}V'(\phi_c) - \frac{H^3}{4\pi^2}\overline{\Pi}_\Delta\,, \tag{57a}$$

$$\dot{\Pi}_\Delta = \frac{1}{3H}V''(\phi_c)\Pi_\Delta\,. \tag{57b}$$

Here, the term $\dot{\Pi}_\Delta(t,\boldsymbol{x})$ on the LHS of (57b) is defined as the Fourier transform of $\dot{\Pi}_\Delta(t,\boldsymbol{k})$ i.e., $\dot{\Pi}_\Delta(t,\boldsymbol{x}) := (2\pi)^{-3}\int \mathrm{d}^3k\,\dot{\Pi}_\Delta(t,\boldsymbol{k})e^{i\boldsymbol{k}\cdot\boldsymbol{x}}$. The same rule applies to other IR variables in the real space as in Equation (A24). Intuitively, this is because the stochastic formalism is formulated in the momentum space, and its Fourier transform provides the stochastic formalism in the real space; see Appendix A for more details.

Equation (57) admits a trivial configuration $\Pi_\Delta(t,\boldsymbol{k}) = 0$ under which we have $H_{\rm HM}=0$, and (57a) becomes $\dot{\phi}_c = -V'(\phi_c)/(3H)$, describing the standard classical time evolution. Now, we are interested in the non-trivial configuration which satisfies (57). In the previous section, we focused on the non-trivial dynamics at the single spatial point $\boldsymbol{x}=\boldsymbol{x}_0$ and it was found that the tunneling configuration was obtained by $\Pi_\Delta(t,\boldsymbol{x}_0) = -\frac{8\pi^2}{3H^4}V'(\phi_c(t,\boldsymbol{x}_0))$. This configuration can be naturally extended to the one in the global picture by considering the following configuration

$$\Pi_\Delta(t,\boldsymbol{k}) = -\frac{8\pi^2}{3H^4}V'(\phi_c(t,\boldsymbol{x}_0))e^{-i\boldsymbol{k}\cdot\boldsymbol{x}_0}\,. \tag{58}$$

From now on, we show that this configuration satisfies a set of Hamilton Equations (57) in a good approximation. For this configuration, we have

$$\Pi_\Delta(t,\boldsymbol{x}) = -\frac{8\pi^2}{3H^4}V'(\phi_c(t,\boldsymbol{x}_0))f(r;t)\,, \tag{59a}$$

$$\dot{\Pi}_\Delta(t,\boldsymbol{x}) = -\frac{8\pi^2}{3H^4}V''(\phi_c(t,\boldsymbol{x}_0))\dot{\phi}_c(t,\boldsymbol{x}_0)f(r;t)\,, \tag{59b}$$

$$\overline{\Pi}_\Delta(t,\boldsymbol{x}) = -\frac{8\pi^2}{3H^4}V'(\phi_c(t,\boldsymbol{x}_0))j_0(k_c(t)r)\,, \tag{59c}$$

where $r := |\boldsymbol{x}-\boldsymbol{x}_0|$, and $f(r;t) := (2\pi)^{-3}\int \mathrm{d}^3k\,\theta(k_c(t)-k)\,e^{i\boldsymbol{k}\cdot(\boldsymbol{x}-\boldsymbol{x}_0)}$. The functions $j_0(k_c(t)r)$ and $f(r;t)$ rapidly oscillate for $r \gg k_c^{-1}(t)$. Hence, they exponentially decay to zero after they are smeared over the Hubble time: for instance, j_0 and f becomes the smooth function after the suitable coarse-graining as[6]

$$\begin{aligned} j_0(k_c(t)r) &\xrightarrow{\text{time c.g.}} W(r;t) := \int \mathrm{d}t' w(t',t) j_0\big(k_c(t')r\big) \approx \begin{cases} 1 & (r \ll k_c^{-1}(t)) \\ 0 & (r \gg k_c^{-1}(t)) \end{cases}, \\ f(r;t) &\xrightarrow{\text{time c.g.}} W_f(r;t) := \int \mathrm{d}t'\, w(t',t) f(r;t') \approx \begin{cases} k_c^3(t)/(6\pi^2) & (r \ll k_c^{-1}(t)) \\ 0 & (r \gg k_c^{-1}(t)) \end{cases}. \end{aligned} \tag{60}$$

Here, we perform the smearing by using a window function $w(t',t)$ which is approximately constant in the domain $|t-t'| \ll H^{-1}$ while it exponentially decays to zero at $|t-t'| \gg$

H^{-1}. We also impose the normalization condition $\int \mathrm{d}t' w(t',t) = 1$. We can choose $w(t',t) = H\pi^{-1/2}\exp[-H^2(t-t')^2]$ for example. Note that the property (60) is based on the behavior $j_0(k_c r) \simeq 1$ and $f(r;t) \simeq k_c^3/(6\pi^2)$ for $r \ll k_c^{-1}$ and the rapid oscillations of $j_0(k_c r)$ and $f_0(r;t)$ for $r \gg k_c^{-1}$. Hence, the property (60) is robust against the choice of $w(t',t)$.

Therefore, substituting Equations (59c) and (60) into Equation (57a) and performing the smearing in time, we obtain

$$\dot{\phi}_c(t,\boldsymbol{x}) = -\frac{1}{3H}\left[V'(\phi_c(t,\boldsymbol{x})) - 2V'(\phi_c(t,\boldsymbol{x}_0))j_0(k_c(t)r)\right] \tag{61a}$$

$$\xrightarrow{\text{time c.g.}} \begin{cases} -V'(\phi_c(t,\boldsymbol{x}))/(3H) & (r \gg k_c^{-1}(t)) \\ V'(\phi_c(t,\boldsymbol{x}_0))/(3H) & (r \ll k_c^{-1}(t)) \end{cases}. \tag{61b}$$

This exhibits the non-trivial dynamics only in the domain $r \lesssim k_c^{-1}$, i.e., a coarse-grained patch centered at a point $\boldsymbol{x}_0$ with a physical radius $(\varepsilon H)^{-1}$. Here, we used $\phi_c(t,\boldsymbol{x}) \simeq \phi_c(t,\boldsymbol{x}_0)$ for $r \ll k_c^{-1}(t)$. In the second line, it is assumed that $V'(\phi_c(t,\boldsymbol{x}_0))$ does not cancel the rapid oscillations of $j_0(k_c(t)r)$ so that their product $V'j_0$ decays exponentially at $r \gg k_c^{-1}$ after the suitable smearing. This assumption is valid thanks to the approximate constancy of super-horizon fluctuations $\phi_c(t,\boldsymbol{k})$ over the Hubble time: $\phi_c(t,\boldsymbol{k}) \simeq \phi_c(t',\boldsymbol{k})$ for $|t-t'| \lesssim H^{-1}$. Adopting the same assumption, from (59a) and (59b), we also obtain the smeared expressions of Π_Δ and $\dot{\Pi}_\Delta$ which turn out to satisfy (57b) under the condition (57a). Hence, we conclude that (59) describes a non-trivial saddle-point solution in a good approximation. Furthermore, after the smearing, we can find $H_{\mathrm{HM}} \approx 0$ for that configuration.

Now, we use the configuration (58) or (59) to obtain the tunneling configuration shown in Figure 4 again. We can calculate the action for this tunneling configuration similarly to (52). By substituting the exact expressions (59) and (61a), we obtain[7]

$$\begin{aligned} I &= -\frac{H^3}{8\pi^2}\int_{t'}^{t_*}\mathrm{d}t\int \mathrm{d}^3x\,\Pi_\Delta(t,\boldsymbol{x})\overline{\Pi}_\Delta(t,\boldsymbol{x}) \\ &= -\frac{8\pi^2}{3H^4}\int_{t'}^{t_*}\mathrm{d}t\,V'(\phi_c(t,\boldsymbol{x}_0))\frac{V'(\phi_c(t,\boldsymbol{x}_0))}{3H}\int \mathrm{d}^3x\,j_0(k_c(t)r)f(r;t) \\ &= -\frac{8\pi^2}{3H^4}\int_{t'}^{t_*}\mathrm{d}t\,\dot{\phi}_c(t,\boldsymbol{x}_0)V'(\phi_c(t,\boldsymbol{x}_0)) = -\frac{8\pi^2}{3H^4}\Delta V\,. \end{aligned} \tag{62}$$

In the first line, we used (57a) to eliminate $\dot{\phi}_c$ from the integrand. In the second line, we substituted the concrete configurations (59). In the third line, we used (61a) and performed the spatial integral as $\int \mathrm{d}^3x\,j_0(k_c(t)r)f(r;t) = 1$. Thus, we reproduced the previous result (52). Our analysis confirms that (62) gives the tunneling probability of a coarse-grained patch with a physical radius $(\varepsilon H)^{-1}$.

It is worth mentioning the time scale of the HM tunneling. We may naively calculate the typical time scale of the HM tunneling as $t_* - t' = \int_{\phi_{\mathrm{false}}}^{\phi_{\mathrm{top}}}\mathrm{d}\phi_c\,\frac{3H}{V'(\phi_c)}$. Here, the spacetime argument of the field is suppressed. However, this integral is in general divergent since $V' = 0$ at both ends of the integral. In the vicinity of the domain where $V' = 0$, we expect that the quantum fluctuations of the field would play an important role. Since the typical size of quantum fluctuations accumulated over the Hubble time is $H/(2\pi)$, we may define the regulated quantity t_{HM} as

$$t_{\mathrm{HM}} := \int_{\phi_{\mathrm{false}}+\frac{H}{2\pi}}^{\phi_{\mathrm{top}}-\frac{H}{2\pi}}\mathrm{d}\phi_c\,\frac{3H}{V'(\phi_c)}\,, \tag{63}$$

and we expect that t_{HM} would correctly characterize the typical time scale of the HM tunneling. In particular, for our potential (42), we have

$$t_{\rm HM} = \frac{3H}{2g^2\alpha^2(1+\beta)}\left[\left(\frac{3+\beta}{1-\beta}\right)\log\left|1-\frac{1-\beta}{H/2\pi\alpha}\right| - \log\left|\frac{1-\frac{2}{H/2\pi\alpha}}{1+\frac{1+\beta}{H/2\pi\alpha}}\right|\right] \sim \frac{1}{H}\cdot\mathcal{O}\Big((H/g\alpha)^2\Big)\,. \tag{64}$$

Since we have $(H/g\alpha)^2 \sim (H^2/V'')_{\phi_{\rm false}\lesssim\phi_c\lesssim\phi_{\rm top}} \gg 1$ for the shallow potential, we conclude that the time scale of HM tunneling is much longer than the Hubble time.

4.2.1. Remark

So far it has been found that starting from (33), the configuration (58) approximately solves Hamilton's Equation (57) and reproduces the previous result (52) when it is substituted into the action. There is actually an important reason behind why we should choose the configuration (58) to evaluate the HM tunneling process.

To see this, it is important to realize an important difference between the current Hamilton Equation (57) and the previous one (48); the equation for ϕ_c now contains $\overline{\Pi}_\Delta$ rather than Π_Δ. Due to this difference, the structures of Hamilton's Equation (57) are understood as follows;

- The equation for ϕ_c (57a) is determined once $\overline{\Pi}_\Delta$ is specified;
- $\overline{\Pi}_\Delta(t,\boldsymbol{x})$ is understood as initial conditions for (57b) since $\overline{\Pi}_\Delta(t,\boldsymbol{x})$ contains only the boundary modes satisfying $k = k_c(t)$. Hence, $\Pi_\Delta(t,\boldsymbol{x})$ is obtained by solving (57b) for a given $\overline{\Pi}_\Delta$ under the condition (57a).

On top of that, substituting Hamilton's equation for ϕ_c into the action, we can rewrite the first line of (62) as

$$I = -\frac{1}{2}\int_{t'}^{t_*}{\rm d}t\int\frac{{\rm d}^3k}{(2\pi)^3}\,\Pi_\Delta(t,\boldsymbol{k})\Pi_\Delta(t,-\boldsymbol{k})\frac{H^2}{2k^3}\delta(t-t_k)\,. \tag{65}$$

The RHS depends only on the value of $\Pi_\Delta(t,\boldsymbol{k})|_{k=k_c(t)}$. Hence, we can evaluate the tunneling action once $\overline{\Pi}_\Delta$ is specified, provided that (65) or equivalently (33) is reliable.

We claim that (33) is valid when $\overline{\Pi}_\Delta$ is chosen so that $\Pi_\Delta(t>t_k,\boldsymbol{k})$ becomes a smooth function in time. Otherwise, it is not justified to ignore the higher-order corrections $\delta H_{\rm higher}$ which are neglected in (33). Intuitively, this states that the perturbation theory tends to be broken down around exotic configurations. When Π_Δ is a smooth function, we can relate $\overline{\Pi}_\Delta$ to Π_Δ after the suitable smearing in time:

$$\overline{\Pi}_\Delta(t,\boldsymbol{x}) \xrightarrow{\text{time c.g.}} \int{\rm d}^3x'\Pi_\Delta(t,\boldsymbol{x}')W(|\boldsymbol{x}-\boldsymbol{x}'|;t) \sim \mathcal{V}\Pi_\Delta(t,\boldsymbol{x})\,. \tag{66}$$

Here, we also used $\Pi_\Delta(t,\boldsymbol{x}) \sim \Pi_\Delta(t,\boldsymbol{x}')$ for $|\boldsymbol{x}-\boldsymbol{x}'| \lesssim k_c^{-1}$ and defined $\mathcal{V} := (4\pi/3)k_c^{-3}(t) \sim \int{\rm d}^3x'\,W(|\boldsymbol{x}-\boldsymbol{x}'|;t)$. We then require that Hamilton's equation for Π_Δ (57b) is satisfied in a good approximation to ensure the validity of (33). This constrains the choice of $\overline{\Pi}_\Delta$. Indeed, the configuration (58) approximately solves (57b) and satisfies the smoothness and henceforth (66) after the smearing. This would be the reason why our analysis with (58) based on (33) can reproduce the correct result.

4.3. On the ε-Independence of the Hawking–Moss Tunneling

In Sections 4.1 and 4.2, the tunneling probability of a coarse-grained patch with a physical radius $(\varepsilon H)^{-1}$ is calculated. Our results coincide with the HM tunneling and are independent of ε.

The ε-independence of the results would be a consequence of the scale independence of the dynamics of light scalar fields at super-horizon scales. To see this, it is useful to notice that a coarse-grained patch of physical radius $(\varepsilon_1 H)^{-1}$ at a time $t = T$ expands to a patch of larger physical radius $(\varepsilon_2 H)^{-1}$ at a later time $t = T+\delta t > T$ with $\varepsilon_2 = \varepsilon_1\exp[-H\delta t] < \varepsilon_1 \ll 1$. The value of the IR field does not evolve from $t = T$ to $T+\delta t$

because the fluctuations of a light scalar field at super-horizon scales are approximately time-independent,

$$\int \frac{\mathrm{d}^3k}{(2\pi)^3}\,\phi_c(t,\boldsymbol{k})e^{i\boldsymbol{k}.\boldsymbol{x}}\theta(k_c(t)-k) \simeq \int \frac{\mathrm{d}^3k}{(2\pi)^3}\,\phi_c(t+\delta t,\boldsymbol{k})e^{i\boldsymbol{k}.\boldsymbol{x}}\theta(k_c(t)-k)\,, \tag{67}$$

unless δt is much longer than H^{-1}. Hence, we can relate the coarse-grained dynamics of different $\varepsilon \ll 1$ by considering the time shift $t \to t+\delta t$ with the value of the IR field being kept fixed. This means that the tunneling probability from $\phi = \phi_{\rm false}$ to $\phi_{\rm true}$ of a patch with physical radius $(\varepsilon H)^{-1}$ should be independent of ε.

5. Coleman–de Luccia Tunneling

In the previous section, the result of the HM instanton was reproduced by using (33). We expect that the Formula (33) can describe not only the HM tunneling but also the CDL tunneling. In other words, we expect a flow line starting from the false vacuum to the bubble configurations as illustrated in Figure 5. In this section, we concretely show an interesting configuration by following the prescription in the previous section.

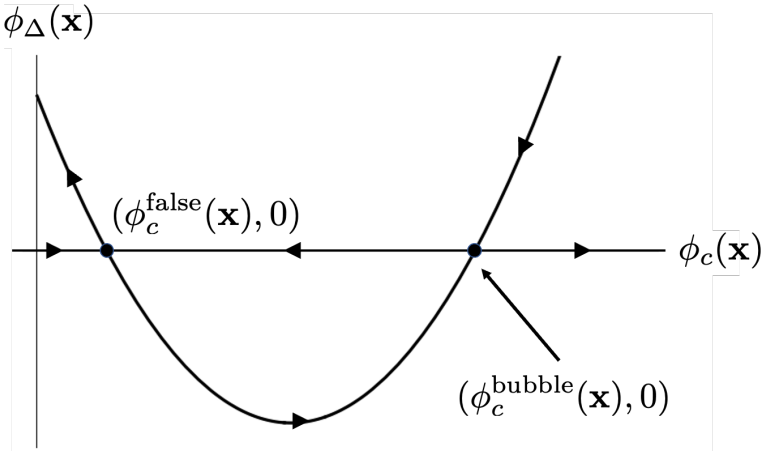

Figure 5. A schematic picture of Hamiltonian flows in the "field" phase space. We expect a flow line which starts from the false vacuum (left intersection) and reaches the bubble configuration (right intersection) through a nonzero $\phi_\Delta(\boldsymbol{x})$ path.

5.1. Coleman–de Luccia Bubble Solution

In the Euclidean method, the CDL instanton is dominant rather than the HM instanton when the potential barrier is steep [28–31]. By taking $\varepsilon \gg 1$, we can study nonperturbative physics at sub-horizon scales such as the formation of a bubble. In this case, $G^{\rm III}$ becomes dominant and the other noises can be ignored in (34). Under this approximation, the exponent of the integrand of (33) is linear in Π_Δ. We can then perform the path integral $\int \mathcal{D}\Pi_\Delta$ in (33), yielding the product of delta functions $\prod_x \delta\left(\dot{\phi}_c - a^{-3}\Pi_c\right)$. These delta functions eliminate the path integral $\int \mathcal{D}\Pi_c$[8]. Furthermore, we change the integration variable as $\phi_\Delta \to -i\phi_\Delta$ in (33), leading to

$$p \simeq \int \mathcal{D}(\phi_c,\phi_\Delta)\exp\left[\int \mathrm{d}^4x\left(a^3\dot{\phi}_\Delta\dot{\phi}_c - H_{\rm CDL}(\phi_c,\phi_\Delta)\right)\right] \tag{68}$$

with appropriate boundary conditions; we consider bubble configurations as boundary conditions later. Here, the Hamiltonian $H_{\rm CDL}$ is defined by

$$H_{\rm CDL}(\phi_c,\phi_\Delta) := -\left(a\nabla^2\phi_c - a^3V'(\phi_c)\right)\phi_\Delta - \frac{a^3}{2}\phi_\Delta(x)\overline{\phi}_\Delta(x)\,, \tag{69}$$

with

$$\overline{\phi}_\Delta(t,\boldsymbol{x}) := \frac{Hk_c^4(t)}{4\pi^2 a(t)} \int \mathrm{d}^3x'\, j_0\big(k_c(t)|\boldsymbol{x}-\boldsymbol{x}'|\big)\phi_\Delta(t,\boldsymbol{x}')\,. \tag{70}$$

We would like to find the appropriate configuration $\overline{\phi}_\Delta$ which describes the tunneling process. Following the choice made in Section 4, let us *suppose* that the appropriate choice is given by the configuration for which the Hamiltonian (69) vanishes:

$$\overline{\phi}_\Delta(x) = 0\,,\ -2(a^{-2}\nabla^2\phi_c - V'(\phi_c))\,. \tag{71}$$

Note that this condition is imposed up to the suitable smearing in time because $\overline{\phi}_\Delta(t,\boldsymbol{x})$ includes only the boundary Fourier mode $k = k_c(t)$. As discussed in Section 4.2.1, ϕ_Δ becomes sufficiently smooth for the appropriate $\overline{\phi}_\Delta$, and hence we also suppose

$$\overline{\phi}_\Delta \sim \frac{H^2\varepsilon}{3\pi}\phi_\Delta(x) \tag{72}$$

after the suitable averaging over the Hubble time, similarly to (66). We use the relation (72) to evaluate the action later. This would work at least for the purpose of estimating the action.

In principle, we do not need to use the estimate (72) in evaluating the action since it is determined once $\overline{\phi}_\Delta$ is specified based on the analogous logic discussed around (65). For this purpose, we need to specify the configurations $\{\phi_\Delta(t,\boldsymbol{k})|_{k=k_c(t)}\}$ in momentum space which result in the sufficiently smooth ϕ_Δ that solves the Hamilton equations. It is not easy to find such appropriate configurations precisely, however. Hence, we leave a more careful analysis on the choice of $\overline{\phi}_\Delta$ for future work. In this study, instead, we focus on how we can proceed with the analysis for the given configuration (71) while adopting the estimate (72) and how the bubble nucleation process could be described in the stochastic approach.

Using the relation (72), the Hamiltonian (69) and the configuration (71) become

$$H_{\mathrm{CDL}} \sim -\Big(a\nabla^2\phi_c - a^3V'(\phi_c)\Big)\phi_\Delta - \frac{H^2\varepsilon}{6\pi}a^3\phi_\Delta^2\,, \tag{73}$$

$$\phi_\Delta(x) = 0\,,\ -\frac{6\pi}{H^2\varepsilon}(a^{-2}\nabla^2\phi_c - V'(\phi_c))\,. \tag{74}$$

Hamilton's equations under the constraints (74) give the following equation of motions for ϕ_c:

$$\begin{aligned}
&\ddot{\phi}_c + 3H\dot{\phi}_c = -(V'(\phi_c) - a^{-2}\nabla^2\phi_c), \quad (\phi_\Delta = 0),\\
&\ddot{\phi}_c + 3H\dot{\phi}_c = V'(\phi_c) - a^{-2}\nabla^2\phi_c, \qquad \Big(\phi_\Delta = -\frac{6\pi}{H^2\varepsilon}(a^{-2}\nabla^2\phi_c - V'(\phi_c))\Big).
\end{aligned} \tag{75}$$

Similar to the previous case (50), the signs of the potential term and the gradient term are flipped in the equation of motion with the non-trivial $\phi_\Delta \neq 0$. Hence, we can expect the tunneling process to be realized. From (68), we find that only the solutions satisfying $\phi_\Delta \neq 0$ contribute to the action. Then, we focus on the second equation in (75).

Interestingly, this equation is the classical equation of motion in the Euclidean anti-de Sitter (AdS) space which is defined by the embedding equation

$$-X_0^2 + X_1^2 + X_2^2 + X_3^2 + X_4^2 = -H^{-2} \tag{76}$$

in five-dimensional Minkowski spacetime

$$\mathrm{d}s^2 = -\mathrm{d}X_0^2 + \mathrm{d}X_1^2 + \mathrm{d}X_2^2 + \mathrm{d}X_3^2 + \mathrm{d}X_4^2\,. \tag{77}$$

In fact, the d'Alembert operator $\partial_t^2 + 3H\partial_t + a^{-2}\nabla^2$ can be obtained from the following induced metrics;

$$ds^2 = dt^2 + e^{2Ht} d\boldsymbol{x}^2 = \frac{1}{H^2\eta^2}(d\eta^2 + d\boldsymbol{x}^2) = H^{-2}(d\rho^2 + \sinh^2\rho\, d\Omega^2)\,, \tag{78}$$

where $d\Omega^2 := d\theta_1^2 + \sin^2\theta_1 d\theta_2^2 + \sin^2\theta_1 \sin^2\theta_2 d\theta_3^2$ and $0 < \rho < \infty, 0 \le \theta_1 \le \pi, 0 \le \theta_2 \le \pi$ and $0 \le \theta_3 \le 2\pi$. The second metric is that in the Poincaré coordinates and the third one is that in the global coordinates. The explicit coordinate transformations are given by

$$\begin{aligned}
X_0 &= \frac{1}{2}\frac{\eta^2 + \boldsymbol{x}^2 + H^{-2}}{-\eta} = H^{-1}\cosh\rho, \\
X_1 &= \frac{x_1}{-H\eta} = H^{-1}\sinh\rho\sin\theta_1\cos\theta_2, \\
X_2 &= \frac{x_2}{-H\eta} = H^{-1}\sinh\rho\sin\theta_1\sin\theta_2\cos\theta_3, \\
X_3 &= \frac{x_3}{-H\eta} = H^{-1}\sinh\rho\sin\theta_1\sin\theta_2\sin\theta_3, \\
X_4 &= \frac{1}{2}\frac{\eta^2 + \boldsymbol{x}^2 - H^{-2}}{-\eta} = H^{-1}\sinh\rho\cos\theta_1.
\end{aligned} \tag{79}$$

For later convenience, we derive the relation between $(\eta, r := |\boldsymbol{x}|)$ and (ρ, σ_1) as

$$-H\eta = \frac{1}{\cosh\rho - \sinh\rho\cos\theta_1}\,, \qquad r = H^{-1}\frac{\sinh\rho\sin\theta_1}{\cosh\rho - \sinh\rho\cos\theta_1}\,. \tag{80}$$

From this, we can check that a point $(\eta, r) = (-H^{-1}, 0)$ is mapped to $\rho = 0$ for any $\theta_1 \in [0, \pi]$. Except for this, there is one-to-one correspondence between points in the (η, r)-plane with $\eta \le 0$ and $r \ge 0$ and points in the (ρ, θ_1)-plane with $\rho > 0$ and $0 \le \theta_1 \le \pi$. On a constant-η slice in the (η, r)-plane, the value of ρ for a given spatial point r is given by

$$\rho = \operatorname{arccosh}\left(\frac{1}{2}\frac{H^2(\eta^2 + r^2) + 1}{-H\eta}\right). \tag{81}$$

This function increases monotonically in r for a given η in the region $r > 0$.

From the global coordinate (78), we see the Euclidean AdS spacetime has $O(4)$ symmetry. Hence, we assume that the field ϕ_c depends only on ρ. Thus, the second equation of (75) reads

$$\frac{d^2\phi_c}{d\rho^2} + \frac{3}{\tanh\rho}\frac{d\phi_c}{d\rho} = \frac{V'(\phi_c)}{H^2}. \tag{82}$$

Note that this is the same equation utilized in the Euclidean method [3,5]. Imposing the boundary conditions [1,3]

$$\lim_{\rho\to\infty}\phi_c = -\alpha, \quad \left.\frac{d\phi_c}{d\rho}\right|_{\rho=0} = 0, \tag{83}$$

we obtain the bubble solutions as shown in Figure 6. Note that the latter condition ensures the continuity of $\partial_\eta\phi_c(\eta, r)$ and $\partial_\eta^2\phi_c(\eta, r)$ at $(H\eta, Hr) = (-1, 0)$.

It is useful to fit the bubble configurations by the following fitting function (Figure 6);

$$\phi_c(\rho) = -\alpha\tanh\mu(\rho - \bar{\rho}), \tag{84}$$

where μ and $\bar{\rho}$ represent the thickness and the position of the bubble wall, respectively. Note that for $\beta \gtrsim 0.6$, the deviation from the true vacuum at $\rho = 0$ becomes significant [26], and the fitting (84) becomes bad.

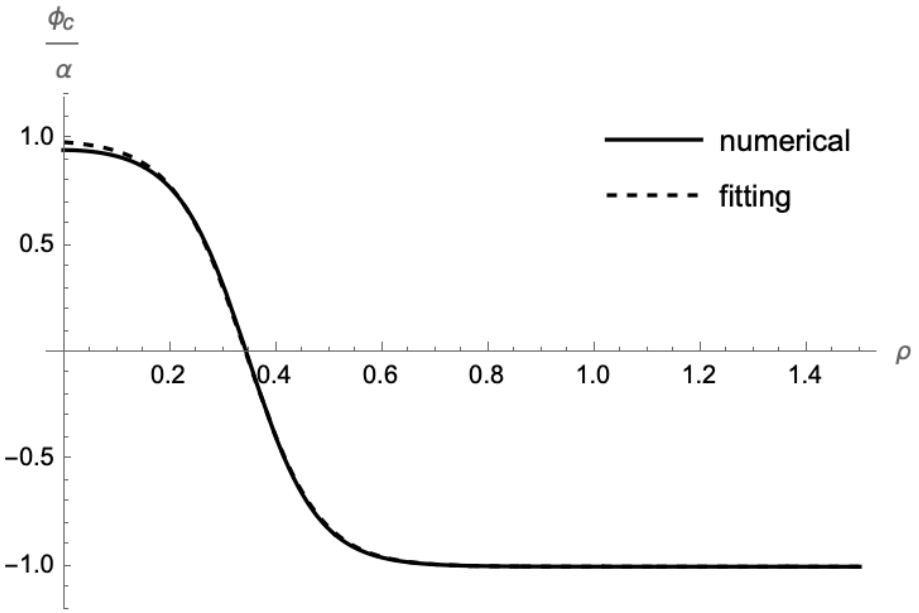

Figure 6. The tunneling configuration for the inhomogeneous field. The solid curve is the numerical solution for $\beta = 0.5$ and $\alpha g/H = \sqrt{140}$. We took the initial conditions as $\phi_c(10^{-15})/\alpha = 1 - 4.98284 \times 10^{-2}$ and $\phi_c'(10^{-15})/\alpha = 0$. The dashed curve is the fitting function (84) where $\mu = 7.32515$ and $\bar{\rho} = 0.34397$.

We also have to examine the boundary conditions in the Hamilton flow. As in the case of HM tunneling, we expect several intersections where $\phi_\Delta = 0$ (Figure 5). Since we have the concrete ϕ_Δ (74) and the bubble configurations (84), it is possible to obtain the curves in the (r, η)-plane on which $\phi_\Delta = 0$. Using (74) and (75), such curves are given by

$$F(\eta, r) := \partial_\eta^2 \phi_c - \frac{2}{\eta} \partial_\eta \phi_c = 0. \tag{85}$$

Note that this is equivalent to solving $a^{-2}\nabla^2 \phi_c - V'(\phi_c) = 0$. Substituting (74) into (85) and using the fitting formula (84), we find four solutions which are expressed as four lines in the (η, r)-plane; two of them are placed at $\eta = -\infty$ with fixed r and $r = \infty$ with fixed η. These correspond to $\rho = \infty$ where $\phi = -\alpha$ (Figure 6). Also, we numerically find other two non-trivial hypersurfaces (Figure 7a). It can be seen that one of the curves is totally spacelike but another is partially timelike. Thus, it seems natural to take the $\eta = -\infty$ curve as an initial time slice on which ϕ is a false vacuum and a totally spacelike non-trivial curve as a final time slice on which the bubble is nucleated. We denote the region between the two spacelike curves as Σ.

As a matter of fact, the configurations on the final time slice has a bubble. It can be checked as follows; the value of ϕ_c at the origin exceeds the top of the potential hill. In the case of Figure 7a where we set $(\beta, \alpha g/H) = (0.5, \sqrt{140})$, we have $\phi_c/\alpha \sim -0.1 > -0.5 = -\beta$ at $Hr = 0, H\eta \sim -0.7$.

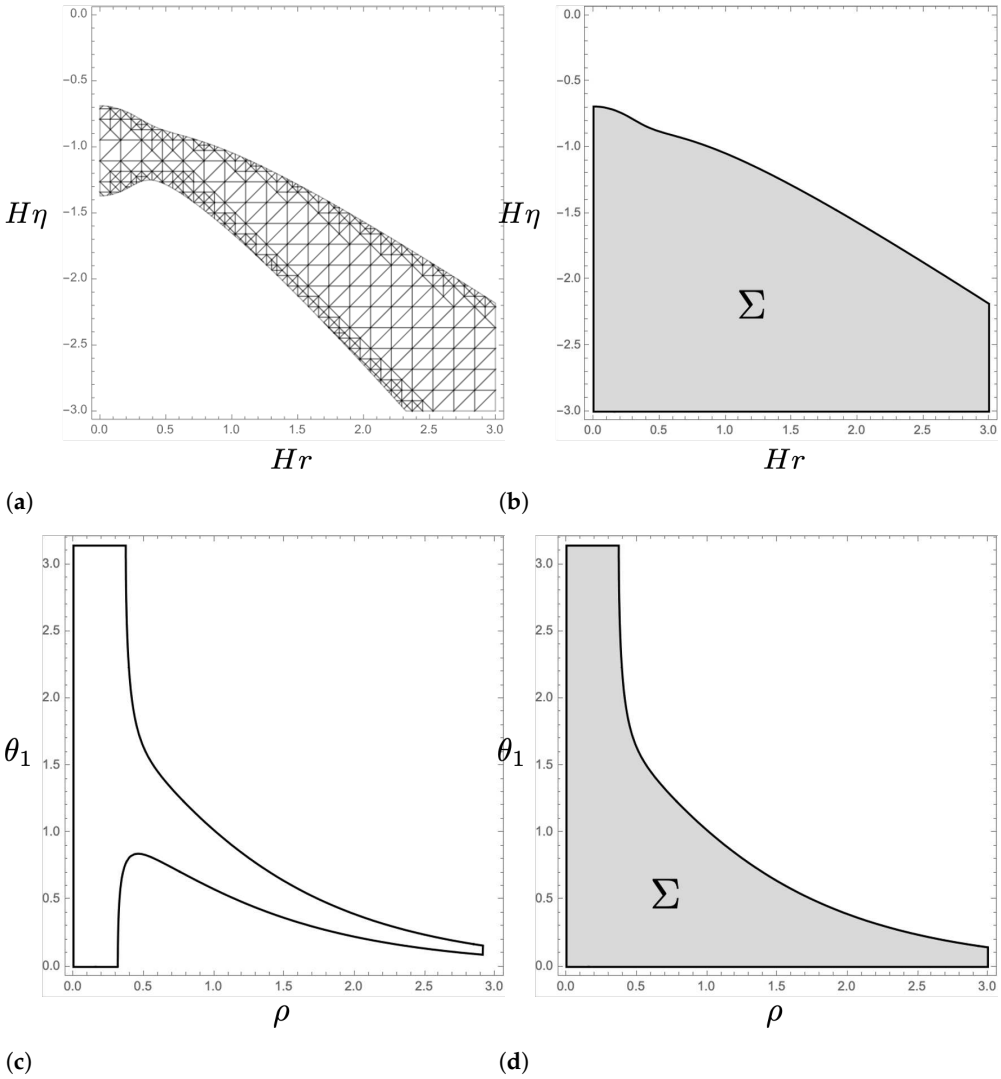

Figure 7. (**a**): The two non-trivial curves on which (85) is satisfied. We inserted the mesh to confirm whether the curves are spacelike or timelike. It can be seen that the upper line is spacelike but the lower one is partially timelike. (**b**): The integration region for (86). There is another spacelike curve at $\eta = -\infty$. (**c**): The two non-trivial curves in (ρ, θ_1) plane. (**d**): The integration region for (86) in the (ρ, θ_1) plane. All plots are with $\beta = 0.5$ and $\alpha g/H = \sqrt{140}$.

Now, we can evaluate the action for the bubble configurations for Σ (Figure 7b,d). We use the fitting function (84) for the numerical integration.

$$\begin{aligned} I &\simeq \int_\Sigma \mathrm{d}^4x \left[-a^3 \phi_\Delta \left(\ddot{\phi}_c + 3H\dot{\phi}_c \right) - H_{\mathrm{CDL}} \right] \\ &= -\frac{6\pi}{H^6 \varepsilon} \int_\Sigma \mathrm{d}\rho \mathrm{d}\theta_1 \mathrm{d}\theta_2 \mathrm{d}\theta_3 \frac{\sin^2\theta_1 \sin\theta_2 \sinh^3\rho}{(\cosh\rho - \sinh\rho\cos\theta_1)^4} \left(\partial_\eta^2 \phi_c - \frac{2}{\eta} \partial_\eta \phi_c \right)^2 \\ &= -\frac{24\pi^2}{H^2 \varepsilon} \int_\Sigma \mathrm{d}\rho \mathrm{d}\theta_1 \sin^2\theta_1 \sinh^3\rho \left[\frac{(\sinh\rho - \cosh\rho\cos\theta_1)^2}{(\cosh\rho - \sinh\rho\cos\theta_1)^2} \frac{\partial^2 \phi_c}{\partial \rho^2} \right. \\ &\quad \left. + \left\{ 3\frac{\sinh\rho - \cosh\rho\cos\theta_1}{\cosh\rho - \sinh\rho\cos\theta_1} + \frac{\sin^2\theta_1}{\tanh\rho(\cosh\rho - \sinh\rho\cos\theta_1)^2} \right\} \frac{\partial \phi_c}{\partial \rho} \right]^2 \\ &:= -\frac{24\pi^2 \alpha^2}{H^2 \varepsilon} \widetilde{I}(\mu, \bar{\rho}). \end{aligned} \tag{86}$$

In the second line, we used $H_{\rm CDL}=0$, (74) and (75). Also, we performed a coordinate transformation $(t,r)\to(\rho,\theta_1)$. In the third line, the following relations were used

$$-\frac{2}{\eta}\frac{\partial\phi_c(\rho)}{\partial\eta}=-\frac{2}{\eta}\frac{\partial\rho}{\partial\eta}\frac{\partial\phi_c(\rho)}{\partial\rho}=2H^2(\cosh\rho-\sinh\rho\cos\theta_1)(\sinh\rho-\cosh\rho\cos\theta_1)\frac{\partial\phi_c(\rho)}{\partial\rho},$$

and

$$\begin{aligned}\frac{\partial^2\phi_c(\rho)}{\partial\eta^2} &= H^2\Bigg[(\sinh\rho-\cosh\rho\cos\theta_1)^2\frac{\partial^2}{\partial\rho^2}\\ &\quad+\Bigg\{(\sinh\rho-\cosh\rho\cos\theta_1)(\cosh\rho-\sinh\rho\cos\theta_1)+\frac{\sin^2\theta_1}{\tanh\rho}\Bigg\}\frac{\partial}{\partial\rho}\Bigg]\phi_c(\rho).\end{aligned}$$

Here, the partial differentiation with respect to η was taken while keeping r constant.

5.2. Discussions

5.2.1. Appropriate Choice of ε

Since our results (86) depend on ε, we need to choose some specific value of ε to predict the tunneling rate. We emphasize that the ε dependence does not imply the pathology of our result. Rather our results should depend on ε because the nonperturbative effects from the UV modes are missed in our formalism, as discussed in Section 3.2. We then choose ε as large as possible to evaluate the tunneling rate.

Our analysis is valid only when the value of ε lies in a certain range. Below, we briefly discuss necessary conditions for ε to justify our analysis.

Lower Bound on ε

We need to choose a sufficiently large ε so that IR fields can describe the bubble configuration. This imposes that $(\varepsilon H)^{-1}$ should be smaller than the typical physical size of the bubble or the bubble wall. This condition is satisfied by taking $\varepsilon\gtrsim\mu$ for our parameter choices.

Upper Bound on ε

Our analysis is based on Equation (33), which is invalid when the quantum fluctuations of IR fields are too large. This imposes an upper bound on ε because the size of the fluctuations in ϕ_c at the scale $k\sim k_c(t)$ is proportional to ε:

$$\delta\phi_c|_{k\sim k_c}:=\left[\int\frac{\mathrm{d}^3k}{(2\pi)^3}\,\delta(\ln(k/k_c(t)))\langle|\hat{\phi}(t,\boldsymbol{k})\big|^2\rangle\right]^{1/2}\approx\frac{k_c/a}{2\pi}=\frac{\varepsilon H}{2\pi}\,,\tag{87}$$

where we assumed $(k_c/a)^2\gg V''(\phi_c)$[9] and approximated ϕ as a massless scalar field.

As discussed in Section 3.2, (33) is justified when the term δH is negligible. Then, we define the ratio $\mathcal{Q}$ of the term δH to the final term on the RHS of (73) as[10]

$$\mathcal{Q}:=\left|\frac{\delta H}{H^2\varepsilon\,a^3\phi_\Delta^2/(6\pi)}\right|_{\phi_\Delta=-\frac{6\pi}{H^2\varepsilon}(a^{-2}\nabla^2\phi_c-V'(\phi_c))}=\frac{3\pi^2}{2\varepsilon^2H^4}\left|V'''(\phi_c)\left(a^{-2}\nabla^2\phi_c-V'(\phi_c)\right)\right|,$$

and we impose $\mathcal{Q}<1$. In the second equality, we used $\delta H=(a^3/24)V'''(\phi_c)\phi_\Delta^3$. Similarly to (87), we can estimate the size of the quantum fluctuations of $a^{-2}\nabla^2\phi$. Then, we estimate $\mathcal{Q}$ at a large ε as $\mathcal{Q}\sim g^2\alpha\varepsilon/H$, where we also used $|V'''(\phi_c)|\sim g^2\alpha$ for $|\phi_c|\lesssim\alpha$. The condition $\varepsilon<H/(g^2\alpha)$ follows from $\mathcal{Q}<1$.

Summary

In summary, it is necessary to choose ε satisfying the following condition to justify our analysis,

$$\mu \lesssim \varepsilon \lesssim \varepsilon_{\max} := H/\left(g^2\alpha\right) \approx 755 \times \left(\frac{1.12\times 10^{-4}}{g}\right)\left(\frac{\sqrt{140}}{g\alpha/H}\right). \tag{88}$$

This suggests that, at least when g is sufficiently tiny, we can reliably choose a large ε. Note that we cannot make the action I given in (86) arbitrarily small even if we take $\varepsilon_{\max} \to \infty$ in the free-theory limit $g \to 0$; for $\varepsilon = \varepsilon_{\max}$, we have $I|_{\varepsilon=\varepsilon_{\max}} \sim -g^{-1}(g\alpha/H)^3\tilde{I}(\mu,\bar{\rho})$. Roughly speaking, the small $g\alpha/H$ corresponds to the bubble radius being larger than the Hubble radius. Since we are interested in the bubble being smaller than the Hubble radius, $g\alpha/H$ cannot be taken small arbitrarily.

A few more comments on the ε-dependence of our results are in order. Our result (86) shows that the value of I becomes larger for smaller choice of ε. This is because the size of the quantum fluctuations of modes $k \sim \varepsilon a(t)H$ is proportional to ε, while the nonperturbative physics caused by UV modes $k > \varepsilon a(t)H$ is truncated in our formalism. However, this interpretation implicitly assumes that the modes $k \sim \varepsilon_{\max} a(t)H$ are relevant for the tunneling process. We expect that this is the case because the kinetic energy of the fluctuations in modes $k \sim \varepsilon_{\max} a(t)H$ is estimated as $(\varepsilon_{\max}H)^4$, which is much smaller than the height of potential barrier $\Delta V \sim g^2\alpha^4$ for our parameter choices.

By contrast, very short scale physics which is insensitive to the detailed structure of $V(\phi)$ near its origin might be irrelevant for the tunneling process. Hence, we expect that the tunneling rate converges to some finite value in the limit $\varepsilon \to \infty$. It would be interesting to see whether the tunneling rate converges to a finite value as ε increases, and if so, from which value of ε this convergence begins.

5.2.2. Hawking–Moss vs. Coleman–de Luccia

From the Formula (33), we derived the two configurations which describe the tunneling from the false vacuum to the true vacuum. One is the HM configuration, and the other is the CDL-like configuration. Using these configurations, we evaluated the probability of the tunneling. Here, we compare these probabilities. Denoting the action (86) and (52) as I_{bubble} and I_{HM}, the ratio of the two actions is given by

$$\gamma := \frac{I_{\text{bubble}}}{I_{\text{HM}}} = \frac{9\alpha^2H^2}{\Delta V\varepsilon}\widetilde{I}(\mu,\bar{\rho}) = \frac{1}{\varepsilon}\frac{108}{(1-\beta)^3(\beta+3)}\frac{H^2}{\alpha^2g^2}\widetilde{I}(\mu,\bar{\rho}) \tag{89}$$

For example, if we choose $\beta = 0.5$ and $\alpha g/H = \sqrt{140}$ (see Figure 6), the fitting parameters become $\mu = 7.32515$ and $\bar{\rho} = 0.34397$, and the ratio becomes $\gamma = 12.9840/\varepsilon$. For these parameters, the upper bound of ϵ is given by (88), and then γ can be smaller than one for an appropriately small g. This means that the CDL bubble configuration is dominant rather than the HM configuration. Results for other parameters are also shown in Table 1.

Table 1. The values of γ for several parameter sets. The first and second ones are potential parameters. The third one is the initial condition for the equation of motion (82). The fourth and fifth ones are fitting parameters for (84). The sixth and seventh ones are the numerical results of (89) and (A48). The last one is the cut-off parameter ϵ for which (89) coincides with (A48).

β	$g^2\alpha^2/H^2$	$1-\phi_c(10^{-15})/\alpha$	μ	$\bar{\rho}$	$\varepsilon\gamma$	γ^E	ϵ_*
0.3	80	4.87210×10^{-5}	6.22563	1.05197	355.089	0.247004	1437.58
0.4	80	5.20273×10^{-3}	5.99645	0.65257	64.1185	0.0909796	704.758
0.5	80	3.89106×10^{-2}	5.63444	0.475247	33.9526	0.0599470	566.376

Table 1. *Cont.*

β	$g^2\alpha^2/H^2$	$1-\phi_c(10^{-15})/\alpha$	μ	$\bar{\rho}$	$\varepsilon\gamma$	γ^E	ϵ_*
0.3	140	3.50945×10^{-4}	8.13990	0.673305	52.2515	0.0486678	1073.64
0.4	140	8.96003×10^{-3}	7.82419	0.459659	19.2912	0.0239903	804.123
0.5	140	4.98284×10^{-2}	7.32515	0.34397	12.9840	0.0172063	754.606

5.2.3. Comparison with the Euclidean Method

We also computed the CDL action in the Euclidean method (Appendix B) and compared the ratios of the CDL action to the HM action (Table 1). For $\varepsilon > \varepsilon_*$, our tunneling process becomes more probable than the one predicted by the Euclidean method. As discussed in Section 5.2.1, we can consistently choose $\varepsilon > \varepsilon_*$ for certain choices of parameters (g, α, β). Perhaps our results may indicate the presence of a tunneling process which is more probable than the Euclidean method.

5.2.4. Bubble Nucleation Hypersurface and the Subsequent Evolution

We found the non-trivial spacelike hypersurface on which the bubble was nucleated (Figure 7a), where the hypersurface was given by the condition $F(\eta, r) = 0$ or equivalently $a^{-2}\nabla^2\phi_c - V'(\phi_c) = 0$. The subsequent evolution was then described by the one shown in the first line of (75), which is the standard classical equation of motion. The configuration on the hypersurface gave the initial data for the classical dynamics after the bubble nucleation.

The field value on the spacelike hypersurface does not reach the true vacuum but rather, it lies between the true vacuum and the top of the potential as mentioned in Section 5.1. This is possible because the location of the hypersurface is defined by the condition $a^{-2}\nabla^2\phi_c - V'(\phi_c) = 0$, where the gradient force is balanced with the potential force. Though it is non-trivial to solve the evolution starting from the general spacelike hypersurfaces, it is desirable to solve it to fully understand the formation of the true-vacuum bubble in our scenario.

We conclude this section by pointing out that our formalism naturally predicts that the condition $\overline{\phi}_\Delta = 0$ (or $\phi_\Delta = 0$ via (72)) defines the hypersurface on which the quantum dynamics is switched to the classical dynamics and the non-trivial field configuration is nucleated. This would be the generic prediction of our formalism that holds true once the appropriate configuration $\overline{\phi}_\Delta$ is specified.

6. Conclusions

We studied the tunneling processes on the de Sitter background by using the stochastic approach. A novel point is that we applied the MSRJD functional integral to the problem. In this formalism, the tunneling rate was obtained by evaluating the functional integral with the saddle-point approximation. Using this method, we investigated both the HM and the CDL tunnelings.

For the HM case, we first analyzed (31), which is the MSRJD functional integral of the stochastic Equation (23) on a single spatial point. We succeeded in deriving the tunneling solution in the "phase space" (Figure 3) which represented the tunneling process from the false vacuum, through the top of the potential hill, and finally to the true vacuum (Figure 4). This solution had natural tunneling boundary conditions which could not be obtained from the Euclidean method. The tunneling rate for this configuration coincided with that of the HM instanton at the leading order. In Section 4.2, we succeeded in re-deriving this result starting from (33), which described the stochastic dynamics in the global region covered by the flat chart. We also estimated the time scale of the HM tunneling as (63), which became much longer than the Hubble time scale. Our analysis clarified the physical picture of the HM instanton, i.e., the HM transition probability represents the transition probability of a coarse-grained patch with a physical radius $(\varepsilon H)^{-1}$. Some technical complications that

arose in dealing with (33) and the way of handling them were remarked on in Section 4.2.1. Physically, these complications were due to the spatial correlations of stochastic noises.

For the CDL case, we found the configurations which described the bubble nucleation process. The tunneling rates for the bubble configurations depended on the cut-off scale dividing IR and UV fields. We argued that this dependence came from the truncation of the nonperturbative effects from UV modes. We also discussed the valid choice of the cut-off scale for which the MSRJD functional integral would be reliable. This consideration was based on the first-principle derivation of the stochastic approach from the Schwinger–Keldysh formalism. With an appropriate cut-off scale, it turned out that the CDL tunneling rate was larger than the HM one for the steep potential barrier. However, as mentioned above (73), it has not yet been investigated if our configuration can really be used for estimating the tunneling action. This aspect would be important for evaluating the tunneling action, being left for future work. Nonetheless, we believe that our study clarifies how we can proceed with the analysis and how the bubble nucleation process could be described in the stochastic approach; for instance, our formalism can naturally define the location of the hypersurface on which the quantum dynamics is switched to the classical dynamics and the non-trivial field configuration is nucleated.

It is interesting to understand the relation between the stochastic approach and the Euclidean method. We compared the CDL tunneling rate in our method with that in the Euclidean method and found the former became larger than the latter for the potential considered with a certain cut-off scale. It would be worth investigating the meaning of this result. In particular, we need to know a precise relation between the CDL instanton and our configuration. Intriguingly, our method is also related to that discussed in [32–36], where the bubble accidentally appears from the initial quantum fluctuations. In our method, however, we assumed that we could neglect the nonperturbative effects from UV modes, the quantum component of the potential of the form $V'''(\phi_c)\phi_\Delta^3$, and that the configuration (74) could be used to estimate the tunneling rate. The first two were summarized into the term δH. We also assumed a fixed-background spacetime. The relaxation of these assumptions would be important to seek the relations among the three methods. It would also be useful to apply our path integral method to the tunneling in flat space and make a comparison with the Euclidean method.

Once this relaxation is achieved, it would also be interesting to apply our method to tunneling phenomena where the backreaction to the background geometry is non-negligible and make comparisons with recently discussed methods. For instance, the formalism of the Wheeler–DeWitt equation [37–39] and the tunneling potential [40] must be related to ours because the HM exponent is reproduced. The tunneling in the black hole spacetime [41,42] is also interesting. In particular, [42] discussed the HM transition with a black hole from the viewpoint of the stochastic approach.

Our method using the saddle-point approximation effectively amounts to solving real-time quantum dynamics, which reduces to Starobinsky's stochastic approach [7,8] at leading order when the super-horizon dynamics in the de Sitter space is considered. However, since our starting point is the Schwinger–Keldysh path integral, which can be formulated in a more generic setup and incorporates all the quantum effects in principle, we believe that our formalism sheds light on further studies of tunneling phenomena from a real-time perspective.

One of the advantages of our method is that it is applicable to a dynamical setup. The application of our method to the inflation models such as the chain inflation [43] and the warm inflation [44] is also intriguing. Using our method, we can study the tunneling process in the inflationary background under dissipation and fluctuations coming from the circumference. We leave these issues for future work.

Author Contributions: Conceptualization, T.M., J.S. and J.T.; methodology, T.M., J.S. and J.T.; software, T.M.; investigation, T.M., J.S. and J.T.; writing—original draft, T.M., J.S. and J.T.; visualization, T.M. All authors have read and agreed to the published version of the manuscript.

Funding: T.M. was supported by JST SPRING, grant number JPMJSP2148 and JSPS KAKENHI grant number JP23KJ1543. J.S. was in part supported by JSPS KAKENHI grant numbers JP17H02894, JP17K18778, JP20H01902, JP22H01220. J.T. is supported by IBS under the project code IBS-R018-D1.

Data Availability Statement: Data are contained within the article.

Conflicts of Interest: The authors declare no conflict of interest.

Appendix A. Stochastic Approach from the First Principle

In this section, we evaluate the generating functional for IR fields $Z[J^{\rm IR}(T)]$ defined in Equation (38) to obtain (39). Note that each step we need to take for evaluating $Z[J^{\rm IR}(T)]$ is summarized in Section 3.2.

Appendix A.1. Path Integral Representation

A path integral representation of $Z[J^{\rm IR}(T)]$ takes the following standard form,

$$Z[J^{\rm IR}(T)] = \int \mathcal{D}(\phi_+,\phi_-,\Pi_+,\Pi_-)\, e^{iJ^{\rm IR}\cdot(\boldsymbol{\phi}_+^{\rm IR}+\boldsymbol{\phi}_-^{\rm IR})/2} \times e^{i(S_H^+ - S_H^-)} \prod_{\boldsymbol{x}} \delta(\phi_+(T,\boldsymbol{x}) - \phi_-(T,\boldsymbol{x}))\Psi_0[\phi_+]\Psi_0^*[\phi_-]\,, \tag{A1}$$

where $\Psi_0[\phi]$ is an initial wave functional. We specify it more concretely in Appendix A.2.1. $S_H^\pm = \int^{t=T} {\rm d}^4x(\Pi^\pm\dot{\phi}^\pm - H[\phi^\pm,\Pi^\pm])$ is a Hamiltonian action. After the rotation of the basis $(X_+,X_-)\to(X_c,X_\Delta) := (\frac{X_+ + X_-}{2}, X_+ - X_-)$ with $X=\phi,\Pi$, (A1) is written as

$$Z[J^{\rm IR}(T)] = \int \mathcal{D}(\phi_c,\phi_\Delta,\Pi_c,\Pi_\Delta)\, e^{iJ^{\rm IR}\cdot\boldsymbol{\phi}_c^{\rm IR}} e^{iS_H[\phi_c,\phi_\Delta,\Pi_c,\Pi_\Delta]} \prod_{\boldsymbol{x}} \delta(\phi_\Delta(T,\boldsymbol{x}))\rho_0[\phi_c,\phi_\Delta]\,. \tag{A2}$$

Here, we defined $S_H[\phi_c,\phi_\Delta,\Pi_c,\Pi_\Delta] := (S_H^+ - S_H^-)|_{(X_+,X_-)\to(X_c,X_\Delta)}$ with $X=\phi,\Pi$. We also defined $\rho_0[\phi_c,\phi_\Delta] := \Psi_0[\phi_c + (\phi_\Delta/2)]\Psi_0^*[\phi_c - (\phi_\Delta/2)]$.

Appendix A.2. Nonperturbative Generating Functional for IR Sector

Now, we explain how to calculate $Z[J^{\rm IR}(T)]$ nonperturbatively in the IR sector. This allows us to capture the nonperturbative physics of the sector $k \le k_c(t)$. Our strategy is to split the integration variables into UV modes $k > k_c(t)$ and IR modes $k \le k_c(t)$ for each time step t, and perform the integration over UV variables to obtain $Z[J^{\rm IR}(T)]$. One may simply split the integration variables $X_a(t,\boldsymbol{k})$[11], where $X=(\phi,\Pi)$ and $a=(c,\Delta)$, by the following replacement in (A2):

$$X_a(t,\boldsymbol{k}) \to \begin{cases} X_a^{\rm IR}(t,\boldsymbol{k}) & (t \ge t_k) \\ X_a^{\rm UV}(t,\boldsymbol{k}) & (t < t_k)\,, \end{cases} \tag{A3}$$

where t_k is defined by the condition $k_c(t_k) = k$. It is then tempting to perform the integration over UV variables $X_a^{\rm UV}$ by using the Schwinger–Keldysh (or *closed-time-path*) formalism. However, the expression obtained from (A2) after the replacement (A3) does not have the product of delta functions $\prod_{\boldsymbol{k}} \delta(\phi_\Delta^{\rm UV}(t_k - 0^+,\boldsymbol{k}))$ at the final time $t = t_k - 0^+$[12]. That is, the time contour for each UV ϕ-variable with modes $0 < k \le k_c(T)$ is not closed at the final time. Hence, the usual Schwinger–Keldysh formalism does not apply for evaluating the integration over UV variables. To resolve this issue, Refs. [22,23] proposed a new way of splitting integration variables. The splitting is given by (A3) for $X=\Pi$, while for ϕ-variable, it is defined by the following rule rather than (A3):

$$\phi_c(t,\boldsymbol{k}) \to \begin{cases} \phi_c^{\rm IR}(t,\boldsymbol{k}) & (t > t_k) \\ \phi_c^{\rm UV}(t,\boldsymbol{k}) & (t \le t_k)\,, \end{cases} \qquad \phi_\Delta(t,\boldsymbol{k}) \to \begin{cases} \phi_\Delta^{\rm IR}(t,\boldsymbol{k}) & (t \ge t_k) \\ \phi_\Delta^{\rm UV}(t,\boldsymbol{k}) & (t < t_k)\,. \end{cases} \tag{A4}$$

In this replacement (A4), the variables $\phi_\Delta^{\rm UV}(t_k, \boldsymbol{k})$ are absent while the variables $\phi_c^{\rm UV}(t_k, \boldsymbol{k})$ are present. Therefore, in the expression obtained from (A2) after the new replacement, the time contour for every UV ϕ-variable including those for modes $\boldsymbol{k}$ with $0 < k \leq k_c(T)$ is closed. This allows us to perform the integration over UV variables based on the Schwinger–Keldysh formalism as we see below. Note that there is no subtlety in the replacement of integration variables $X_a(t, \boldsymbol{k})$ for a zero mode $k = 0$ and those for deep UV modes $k > k_c(T)$: in both replacement rules mentioned above, they are simply replaced by IR variables $X_a^{\rm IR}(t, \boldsymbol{k})$ and UV variables $X_a^{\rm UV}(t, \boldsymbol{k})$, respectively. The time contours for them are closed thanks to the product of delta functions in the original expression (A2).

After the new replacement, the term $S_H[\phi_c, \phi_\Delta, \Pi_c, \Pi_\Delta]$ in the exponent of (A2) is decomposed into three pieces: purely IR terms $S_H^{\rm IR} := S_H[\phi_c^{\rm IR}, \phi_\Delta^{\rm IR}, \Pi_c^{\rm IR}, \Pi_\Delta^{\rm IR}]$, purely UV terms $S_H^{\rm UV} := S_H[\phi_c^{\rm UV}, \phi_\Delta^{\rm UV}, \Pi_c^{\rm UV}, \Pi_\Delta^{\rm UV}]$ and the remaining IR–UV mixing terms $S_{\rm mixed}$:

$$S_H[\phi_c, \phi_\Delta, \Pi_c, \Pi_\Delta] \to S_H^{\rm IR} + S_H^{\rm UV} + S_{\rm mixed}\,. \tag{A5}$$

In terms of these quantities, $Z[J^{\rm IR}(T)]$ can be formally written as [22,23]

$$\begin{aligned} Z[J^{\rm IR}(T)] = \int \mathcal{D}(\phi_c^{\rm IR}, \phi_\Delta^{\rm IR}, \Pi_c^{\rm IR}, \Pi_\Delta^{\rm IR})\, e^{i\boldsymbol{J}^{\rm IR}\cdot\boldsymbol{\phi}_c^{\rm IR}} e^{iS_H^{\rm IR}} e^{i\Gamma} \\ \times \prod_{k\leq k_c(T)} \delta(\phi_\Delta^{\rm IR}(T, \boldsymbol{k})) \prod_{0<k\leq k_c(T)} \delta(\phi_c^{\rm IR}(t_k, \boldsymbol{k})), \end{aligned} \tag{A6}$$

where $i\Gamma$ is the effective action for IR fields,

$$e^{i\Gamma} := \int \mathcal{D}(\phi_c^{\rm UV}, \phi_\Delta^{\rm UV}, \Pi_c^{\rm UV}, \Pi_\Delta^{\rm UV})\, e^{i(S_H^{\rm UV}+S_{\rm mixed})} \prod_{k>0} \delta(\phi_\Delta^{\rm IR}(t_f(k), \boldsymbol{k}))\rho_0[\phi_c^{\rm UV}, \phi_\Delta^{\rm UV}; \phi_c^{\rm IR}, \phi_\Delta^{\rm IR}]\,, \tag{A7}$$

with $t_f(k) := \min[T, t_k]$. Here, $\rho_0[\phi_c, \phi_\Delta] \to \rho_0[\phi_c^{\rm UV}, \phi_\Delta^{\rm UV}; \phi_c^{\rm IR}, \phi_\Delta^{\rm IR}]$ due to the replacement of variables. The IR variables $(\phi_c^{\rm IR}, \phi_\Delta^{\rm IR})$ in the argument of ρ_0 contain only a zero mode. Since the time path for each UV ϕ-variable is closed in (A7), we can calculate $i\Gamma$ perturbatively as usual by writing the connected diagrams with n external IR fields that are connected by UV propagators. The diagrammatic rules such as vertex factors and symmetry factors follow the standard rules of the Scheinger–Keldysh formalism for given vertexes in $S_H^{\rm UV} + S_{\rm mixed}$.

Interestingly, due to the non-trivial replacement rule (A4), the $\Pi\dot{\phi}$ terms in S_H also contribute to $S_{\rm mixed}$ [11,22–24]. Referring to such contributions and the remaining terms in $S_{\rm mixed}$ as $S_{\rm tr}$ and $S_{\text{mix-int}}$, respectively, we have $S_{\rm mixed} = S_{\rm tr} + S_{\text{mix-int}}$ with [13]

$$S_{\rm tr} := \int_{-\infty}^{T} {\rm d}t \int \frac{{\rm d}^3k}{(2\pi)^3} \delta(t - t_k) \left[\phi_\Delta^{\rm IR}(t, -\boldsymbol{k})\Pi_c^{\rm UV}(t, \boldsymbol{k}) - \Pi_\Delta^{\rm IR}(-\boldsymbol{k}, t)\phi_c^{\rm UV}(t, \boldsymbol{k})\right]. \tag{A8}$$

The bi-linear vertexes exist only at the UV→IR transition time t_k for given modes with $0 < k \leq k_c(T)$. Physically, these vertexes set the initial fluctuations for such modes in (A6).

Appendix A.2.1. Integrate out Short-Wavelength Modes

Now, we calculate $i\Gamma$ perturbatively by specifying the setup more concretely. We organize the perturbation theory around the false vacuum state ρ_0 for which the expectation value of the zero mode is $\phi_{\rm false}$. We assume that the fluctuations of zero modes are tiny enough so that the couplings between zero-mode fluctuations and those of nonzero modes $k > 0$ are switched off in the past infinity $t = -\infty$. We then take the initial state of nonzero modes to be the Bunch–Davies vacuum state for a free field, where the time evolution of a free field is defined by the quadratic action expanded around the homogeneous background $\phi_{\rm false}$. These assumptions can be implemented by writing the initial quantum state as

$$\rho_0[\phi_c^{\rm UV}, \phi_\Delta^{\rm UV}; \phi_c^{\rm IR}, \phi_\Delta^{\rm IR}] = \rho_{\rm BD}[\phi_c^{\rm UV}, \phi_\Delta^{\rm UV}; \phi_{\rm false}]\, \rho_0[\phi_c^{\rm IR} - \phi_{\rm false}, \phi_\Delta^{\rm IR}] \tag{A9}$$

which is properly normalized as

$$1 = \prod_{k>0} \int \mathrm{d}\phi_c^{\mathrm{UV}}(-\infty, \boldsymbol{k}) \int \mathrm{d}\phi_\Delta^{\mathrm{UV}}(-\infty, \boldsymbol{k})\, \rho_{\mathrm{BD}}[\phi_c^{\mathrm{UV}}, \phi_\Delta^{\mathrm{UV}}; \phi_{\mathrm{false}}]$$
$$= \int \mathrm{d}\phi_c^{\mathrm{IR}}(-\infty, \boldsymbol{0}) \int \mathrm{d}\phi_\Delta^{\mathrm{IR}}(-\infty, \boldsymbol{0})\, \rho_0[\phi_c^{\mathrm{IR}} - \phi_{\mathrm{false}}, \phi_\Delta^{\mathrm{IR}}]\,. \tag{A10}$$

$\rho_{\mathrm{BD}}[\phi_c^{\mathrm{UV}}, \phi_\Delta^{\mathrm{UV}}; \phi_{\mathrm{false}}]$ is the density matrix for nonzero modes. An initial state for the zero mode is given by $\rho_0[\phi_c^{\mathrm{IR}} - \phi_{\mathrm{false}}, \phi_\Delta^{\mathrm{IR}}]$, for which we have

$$\langle \Psi(-\infty)|\, \hat{\phi}(\boldsymbol{k} = \boldsymbol{0})\, |\Psi(-\infty)\rangle = \int \mathrm{d}\phi_c^{\mathrm{IR}} \rho_0[\phi_c^{\mathrm{IR}} - \phi_{\mathrm{false}}, \phi_\Delta^{\mathrm{IR}}] \phi_c^{\mathrm{IR}} = \phi_{\mathrm{false}} (2\pi)^3 \delta(\boldsymbol{0})\,. \tag{A11}$$

Combining this with $\langle \Psi(-\infty)|\, \hat{\phi}(\boldsymbol{k})\, |\Psi(-\infty)\rangle = 0$ for nonzero modes $k > 0$, we have

$$\langle \Psi(-\infty)|\, \hat{\phi}(\boldsymbol{k})\, |\Psi(-\infty)\rangle = \phi_{\mathrm{false}} (2\pi)^3 \delta(\boldsymbol{k})\,. \tag{A12}$$

Hence, the VEV of the IR field $\hat{\phi}^{\mathrm{IR}}(t, \boldsymbol{x})$ in the past infinity $t = -\infty$ is given by ϕ_{false}.

The interaction vertexes for calculating $i\Gamma$ are the bi-linear vertexes (A8) and nonlinear vertexes coming from interacting potential $V(\phi)$. We assume that the potential is sufficiently flat under the region we are interested in. It is then natural to separate $i\Gamma$ into the leading-order pieces and higher-order terms in the coupling constant as follows,

$$e^{i\Gamma} = \rho_0[\phi_c^{\mathrm{IR}} - \phi_{\mathrm{false}}, \phi_\Delta^{\mathrm{IR}}]\, e^{i\Gamma_{\mathrm{LO}}^{k>0}} e^{-i\int \mathrm{d}^4x\, \delta H_{\mathrm{higher}}}\,,$$
$$e^{i\Gamma_{\mathrm{LO}}^{k>0}} := \int \mathcal{D}(\phi_c^{\mathrm{UV}}, \phi_\Delta^{\mathrm{UV}}, \Pi_c^{\mathrm{UV}}, \Pi_\Delta^{\mathrm{UV}})\, e^{iS_{H,\mathrm{free}}^{\mathrm{UV}} + S_{\mathrm{tr}}} \prod_{k>0} \delta(\phi_\Delta^{\mathrm{IR}}(t_f(k), \boldsymbol{k})) \rho_{\mathrm{BD}}[\phi_c^{\mathrm{UV}}, \phi_\Delta^{\mathrm{UV}}; \phi_{\mathrm{false}}]\,. \tag{A13}$$

Here, $S_{H,\mathrm{free}}^{\mathrm{UV}}[\phi_c^{\mathrm{UV}}, \phi_\Delta^{\mathrm{UV}}, \Pi_c^{\mathrm{UV}}, \Pi_\Delta^{\mathrm{UV}}; \phi_{\mathrm{false}}]$ is the free part of the Hamiltonian action defined around the false vacuum as explained above. Higher-order corrections to Γ in the coupling constant are represented by the term $\delta H_{\mathrm{higher}}$, which can be evaluated perturbatively. We have $\delta H_{\mathrm{higher}} = 0$ at the leading order.

To calculate $i\Gamma_{\mathrm{LO}}^{k>0}$ by writing down the connected diagrams with external IR fields, we only need to consider the bi-linear vertexes S_{tr} given in (A8). The number of diagrams are only four, and $i\Gamma_{\mathrm{LO}}^{k>0}$ can be calculated as [22,23]

$$i\Gamma_{\mathrm{LO}}^{k>0} = \frac{-1}{2} \int \mathrm{d}t \int \mathrm{d}t' \int \frac{\mathrm{d}^3k}{(2\pi)^3}\, X_\alpha(t, \boldsymbol{k}) g^{\alpha\beta}(t, t', k) X_\beta(t', -\boldsymbol{k})$$
$$= \frac{-1}{2} \int \mathrm{d}^4x \int \mathrm{d}^4x'\, X_\alpha(x) G^{\alpha\beta}(x, x') X_\beta(x')\,. \tag{A14}$$

Here, the Greek indices $\alpha, \beta = (\phi, \Pi)$ label the IR-Δ fields: $(X_\phi, X_\Pi) = (\Pi_\Delta^{\mathrm{IR}}, -\phi_\Delta^{\mathrm{IR}})$. Substituting Equation (A13) into (A6), we find

$$Z[J^{\mathrm{IR}}(T)] = \int \mathcal{D}(\phi_c^{\mathrm{IR}}, \phi_\Delta^{\mathrm{IR}}, \Pi_c^{\mathrm{IR}}, \Pi_\Delta^{\mathrm{IR}})\, e^{i\boldsymbol{J}^{\mathrm{IR}}\cdot\boldsymbol{\phi}_c^{\mathrm{IR}}} \rho_0[\phi_c^{\mathrm{IR}} - \phi_{\mathrm{false}}, \phi_\Delta^{\mathrm{IR}}]\, e^{i(S_H^{\mathrm{IR}} + \Gamma_{\mathrm{LO}}^{k>0})} e^{-i\int \mathrm{d}^4x\, \delta H_{\mathrm{higher}}}$$
$$\times \prod_{k \le k_c(T)} \delta(\phi_\Delta^{\mathrm{IR}}(T, \boldsymbol{k})) \prod_{0<k\le k_c(T)} \delta(\phi_c^{\mathrm{IR}}(t_k, \boldsymbol{k}))\,. \tag{A15}$$

Now, we introduce $i\Gamma_{k=0}$ as

$$e^{i\Gamma_{k=0}[\phi_\Delta^{\mathrm{IR}}, \Pi_\Delta^{\mathrm{IR}}]} := \int \mathrm{d}\phi_c^{\mathrm{IR}} \rho_0[\phi_c^{\mathrm{IR}} - \phi_{\mathrm{false}}, \phi_\Delta^{\mathrm{IR}}] e^{-i\Pi_\Delta^{\mathrm{IR}}(\phi_c^{\mathrm{IR}} - \phi_{\mathrm{false}}(2\pi)^3\delta(\boldsymbol{0}))}\,. \tag{A16}$$

By definition, we have

$$\begin{aligned}&\int \mathrm{d}\phi_c^{\mathrm{IR}} \rho_0[\phi_c^{\mathrm{IR}} - \phi_{\mathrm{false}}, \phi_\Delta^{\mathrm{IR}}]\, e^{-i\Pi_\Delta^{\mathrm{IR}}\left(\phi_c^{\mathrm{IR}} - \phi_{\mathrm{false}}(2\pi)^3\delta(\mathbf{0})\right)} \\ &= \int \mathrm{d}\phi_c^{\mathrm{IR}}\, e^{-i\Pi_\Delta^{\mathrm{IR}}\phi_c^{\mathrm{IR}}} e^{i\Gamma_{k=0}[\phi_\Delta^{\mathrm{IR}}, \Pi_\Delta^{\mathrm{IR}}]} \delta\left(\phi_c^{\mathrm{IR}} - \phi_{\mathrm{false}}(2\pi)^3\delta(\mathbf{0})\right). \end{aligned} \tag{A17}$$

Substituting (A17) into (A15), we find

$$\begin{aligned}Z[J^{\mathrm{IR}}(T)] = \int \mathcal{D}(\phi_c^{\mathrm{IR}}, \phi_\Delta^{\mathrm{IR}}, \Pi_c^{\mathrm{IR}}, \Pi_\Delta^{\mathrm{IR}})\, e^{iJ^{\mathrm{IR}}\cdot\boldsymbol{\phi}_c^{\mathrm{IR}}}\, e^{i(S_H^{\mathrm{IR}} + \Gamma_{\mathrm{LO}}^{k>0} + \Gamma_{k=0})} e^{-i\int \mathrm{d}^4x\, \delta H_{\mathrm{higher}}} \\ \times \prod_{k\le k_c(T)} \delta(\phi_\Delta^{\mathrm{IR}}(T,\boldsymbol{k}))\delta(\phi_c^{\mathrm{IR}}(t_k,\boldsymbol{k}) - \phi_{\mathrm{false}}(2\pi)^3\delta(\boldsymbol{k}))\,, \end{aligned} \tag{A18}$$

by defining $t_k|_{k=0} = -\infty$.

Appendix A.2.2. Long-Wavelength Sector

For later convenience, let us focus on the term $\int \mathrm{d}t\, \Pi_c^{\mathrm{IR}}(t,\boldsymbol{k})\dot{\phi}_\Delta^{\mathrm{IR}}(t,-\boldsymbol{k})$ in S_H^{IR}. We use the following trick to perform the integration by parts:

$$\begin{aligned}&\delta(\phi_\Delta^{\mathrm{IR}}(T,\boldsymbol{k}))\, e^{i\int_{t_k}^{T} \mathrm{d}t\, \Pi_c^{\mathrm{IR}}(t,\boldsymbol{k})\dot{\phi}_\Delta^{\mathrm{IR}}(t,-\boldsymbol{k})} \\ &= \delta(\phi_\Delta^{\mathrm{IR}}(T,\boldsymbol{k})) \int \mathrm{d}\Pi_c^{\mathrm{IR}}(t_k - 0^+,\boldsymbol{k})\, e^{i\int_{t_k-0^+}^{T} \mathrm{d}t\, \Pi_c^{\mathrm{IR}}(t,\boldsymbol{k})\dot{\phi}_\Delta^{\mathrm{IR}}(t,-\boldsymbol{k})} \delta(\Pi_c^{\mathrm{IR}}(t_k - 0^+,\boldsymbol{k})) \\ &= \delta(\phi_\Delta^{\mathrm{IR}}(T,\boldsymbol{k})) \int \mathrm{d}\Pi_c^{\mathrm{IR}}(t_k - 0^+,\boldsymbol{k})\, e^{-i\int_{t_k-0^+}^{T} \mathrm{d}t\, \dot{\Pi}_c^{\mathrm{IR}}(t,\boldsymbol{k})\phi_\Delta^{\mathrm{IR}}(t,-\boldsymbol{k})} \delta(\Pi_c^{\mathrm{IR}}(t_k - 0^+,\boldsymbol{k}))\,. \end{aligned} \tag{A19}$$

Thanks to this trick, (A18) can be written as

$$\begin{aligned}Z[J^{\mathrm{IR}}(T)] = \int \mathcal{D}(\phi_c^{\mathrm{IR}}, \phi_\Delta^{\mathrm{IR}}, \Pi_c^{\mathrm{IR}}, \Pi_\Delta^{\mathrm{IR}}) \int \widetilde{\mathcal{D}}\Pi_c^{\mathrm{IR}}\, e^{iJ^{\mathrm{IR}}\cdot\boldsymbol{\phi}_c^{\mathrm{IR}}}\, e^{i(S_{H,(d)}^{\mathrm{IR}} + S_{H,(s)}^{\mathrm{IR}} + \Gamma_{\mathrm{LO}}^{k>0} + \Gamma_{k=0})} e^{-i\int \mathrm{d}^4x\, \delta H_{\mathrm{higher}}} \\ \times \prod_{k\le k_c(T)} \delta(\phi_\Delta^{\mathrm{IR}}(T,\boldsymbol{k}))\delta(\phi_c^{\mathrm{IR}}(t_k,\boldsymbol{k}) - \phi_{\mathrm{false}}(2\pi)^3\delta(\boldsymbol{k}))\delta(\Pi_c^{\mathrm{IR}}(t_k - 0^+,\boldsymbol{k}))\,, \end{aligned} \tag{A20}$$

where $\widetilde{\mathcal{D}}\Pi_c^{\mathrm{IR}} := \prod_{k\le k_c(T)} \mathrm{d}\Pi_c^{\mathrm{IR}}(t_k - 0^+,\boldsymbol{k})$. Below, we simply omit this integration measure to simplify the notation. We also decompose S_H^{IR} as $S_H^{\mathrm{IR}} = S_{H,(d)}^{\mathrm{IR}} + S_{H,(s)}^{\mathrm{IR}}$ up to the boundary terms, which vanish thanks to the trick (A19) as

$$S_{H,(d)}^{\mathrm{IR}} = \int \mathrm{d}^4x \left[\Pi_\Delta^{\mathrm{IR}}\left(\dot{\phi}_c^{\mathrm{IR}} - a^{-3}\Pi_c^{\mathrm{IR}}\right) - \phi_\Delta^{\mathrm{IR}}\left(\dot{\Pi}_c^{\mathrm{IR}} - a(t)\nabla^2\phi_c^{\mathrm{IR}} + a^3(t)\, V'(\phi_c^{\mathrm{IR}})\right)\right], \tag{A21}$$

$$S_{H,(s)}^{\mathrm{IR}} = -\int \mathrm{d}^4x\, a^3(t) \left[V(\phi_c^{\mathrm{IR}} + (\phi_\Delta^{\mathrm{IR}}/2)) - V(\phi_c^{\mathrm{IR}} - (\phi_\Delta^{\mathrm{IR}}/2)) - V'(\phi_c^{\mathrm{IR}})\phi_\Delta^{\mathrm{IR}}\right]. \tag{A22}$$

Here, the spacetime argument of IR variables are omitted. We introduce the IR variables and their time derivatives as

$$X^{\mathrm{IR}}(t,\boldsymbol{x}) := \int \frac{\mathrm{d}^3k}{(2\pi)^3}\, \theta(k_c(t) - k)\, X^{\mathrm{IR}}(t,\boldsymbol{k})\, e^{i\boldsymbol{k}.\boldsymbol{x}}\,, \tag{A23}$$

$$\dot{X}^{\mathrm{IR}}(t,\boldsymbol{x}) := \int \frac{\mathrm{d}^3k}{(2\pi)^3}\, \theta(k_c(t) - k)\, \dot{X}^{\mathrm{IR}}(t,\boldsymbol{k})\, e^{i\boldsymbol{k}.\boldsymbol{x}}\,, \tag{A24}$$

where X^{IR} represents the IR variables: $X^{\mathrm{IR}} = (\phi_c^{\mathrm{IR}}, \phi_\Delta^{\mathrm{IR}}, \Pi_c^{\mathrm{IR}}, \Pi_\Delta^{\mathrm{IR}})$. Precisely speaking, for $X^{\mathrm{IR}} = \Pi_c^{\mathrm{IR}}$, we should replace $k_c(t)$ by $k_c(t + 0^+)$ so that we have $k_c(t) = k$ at $t = t_k - 0^+$. One may be concerned about the subtlety of the time derivatives $\dot{\phi}_c^{\mathrm{IR}}(t,\boldsymbol{x})$ and $\dot{\Pi}_c^{\mathrm{IR}}(t,\boldsymbol{x})$ in (A21): in general we have $\dot{X}^{\mathrm{IR}}(t,\boldsymbol{x}) \neq \frac{\partial}{\partial t}(X^{\mathrm{IR}}(t,\boldsymbol{x}))$, where the LHS is defined by (A24),

due to the presence of a time-dependent step function. However, there is no subtlety thanks to the initial conditions for all IR modes $k \leq k_c(T)$ of the form

$$\phi_c^{\rm IR}(t_k, \boldsymbol{k}) = \phi_{\rm false}(2\pi)^3\delta(\boldsymbol{k})\,, \qquad \Pi_c^{\rm IR}(t_k - 0^+, \boldsymbol{k}) = 0\,, \tag{A25}$$

which are imposed by the delta functions in the final line in (A20). The corresponding conditions in the real space for all $\boldsymbol{x}$ are

$$\dot{X}^{\rm IR}(t,\boldsymbol{x}) = \partial_t(X^{\rm IR}(t,\boldsymbol{x})) \quad \text{for} \quad X^{\rm IR} = (\phi_c^{\rm IR},\, \Pi_c^{\rm IR})\,, \tag{A26a}$$

$$\phi_c^{\rm IR}(-\infty,\boldsymbol{x}) = \phi_{\rm false}\,, \quad \Pi_c^{\rm IR}(-\infty,\boldsymbol{x}) = 0\,. \tag{A26b}$$

To implement these conditions in the path integral, we define $\delta[\mathcal{C}_{\rm ini}]$ by (40b) with

$$\delta[\mathcal{C}_{\rm detail}] := \prod_{-\infty\leq t\leq T}\prod_{X^{\rm IR}=(\phi_c^{\rm IR},\Pi_c^{\rm IR})}\prod_{\boldsymbol{x}}\delta\Big(\dot{X}^{\rm IR}(t,\boldsymbol{x}) - \partial_t(X^{\rm IR}(t,\boldsymbol{x}))\Big)\,. \tag{A27}$$

We find from Equations (37) and (A20) that the transition probability can be written in terms of the path integral as

$$p(\{\phi^{\rm IR}(T,\boldsymbol{x})\}_{T,\boldsymbol{x}\in\mathcal{D}}) = \int \mathcal{D}(\phi_c^{\rm IR},\phi_\Delta^{\rm IR},\Pi_c^{\rm IR},\Pi_\Delta^{\rm IR})\; e^{i\mathcal{S}}e^{i\Gamma_{k=0}}\delta[\mathcal{C}_{\rm fin}]\delta[\mathcal{C}_{\rm ini}]\,, \tag{A28}$$

where $\delta[\mathcal{C}_{\rm fin}]$ is defined in (40a), and the term $\mathcal{S}$ in the exponent is given by

$$\mathcal{S} = (S^{\rm IR}_{H,(d)} + S^{\rm IR}_{H,(s)} + \Gamma^{k>0}_{\rm LO}) - \int {\rm d}^4x\,\delta H_{\rm higher} \tag{A29}$$

which agrees with the definition of $\mathcal{S}$ given in (41). When the zero-mode fluctuations are negligible, we can set $\Gamma_{k=0} = 0$. This is the setup adopted in the main text. Then, (A28) coincides with (39).

Appendix A.3. Stochastic Interpretation of the Tunneling

It is useful to see how the stochastic equations emerge as a consequence of performing the path integral over IR variables nonperturbatively. This leads to the stochastic interpretation of the tunneling probability. A final result of this section is (A39).

For simplicity, let us ignore higher-order corrections $\delta H_{\rm higher}$ for a while. We start by introducing the auxiliary fields (ξ_ϕ, ξ_Π) as

$$e^{i\left(\Gamma^{k>0}_{\rm LO}+\Gamma_{k=0}+S^{\rm IR}_{H,(s)}\right)} = \int \mathcal{D}(\xi_\phi,\xi_\Pi)\,P[\xi_\phi,\xi_\Pi]e^{i\int {\rm d}^4x\left(\xi_\Pi(x)\phi^{\rm IR}_\Delta(x) - \xi_\phi(x)\Pi^{\rm IR}_\Delta(x)\right)}\,. \tag{A30}$$

We substitute (A30) into (A20). Then, the exponent becomes linear in $\phi^{\rm IR}_\Delta(t,\boldsymbol{k})$ or $\Pi^{\rm IR}_\Delta(t,\boldsymbol{k})$ with $t_0 \leq t < T$:

$$\begin{aligned} Z[J^{\rm IR}(T)] \simeq \int \mathcal{D}(\phi_c^{\rm IR},\phi_\Delta^{\rm IR},\Pi_c^{\rm IR},\Pi_\Delta^{\rm IR}) \int \widetilde{\mathcal{D}}\Pi_c^{\rm IR}\, e^{iJ^{\rm IR}\cdot\boldsymbol{\phi}_c^{\rm IR}} \int \mathcal{D}(\xi_\phi,\xi_\Pi)\,P[\xi_\phi,\xi_\Pi] \\ \times \exp\left\{ i\int_{-\infty}^{T}{\rm d}t\int\frac{{\rm d}^3k}{(2\pi)^3}\left[\Pi^{\rm IR}_\Delta(t,-\boldsymbol{k})\mathcal{L}_\phi(t,\boldsymbol{k}) - \phi^{\rm IR}_\Delta(t,-\boldsymbol{k})\mathcal{L}_\Pi(t,\boldsymbol{k})\right]\Theta(k_c(t)-k)\right\} \\ \times \prod_{k\leq k_c(T)}\delta(\phi^{\rm IR}_\Delta(T,\boldsymbol{k}))\delta(\phi^{\rm IR}_c(t_k,\boldsymbol{k}) - \phi_{\rm false}(2\pi)^3\delta(\boldsymbol{k}))\delta(\Pi^{\rm IR}_c(t_k-0^+,\boldsymbol{k}))\,, \end{aligned} \tag{A31}$$

where

$$\mathcal{L}_\phi(t,\boldsymbol{k}) := \dot{\phi}^{\rm IR}_c(t,\boldsymbol{k}) - a^{-3}(t)\Pi^{\rm IR}_c(t,\boldsymbol{k}) - \xi_\phi(t,\boldsymbol{k})\,, \tag{A32a}$$

$$\mathcal{L}_\pi(t,\boldsymbol{k}) := \dot{\Pi}^{\rm IR}_c(t,\boldsymbol{k}) + a(t)k^2\phi^{\rm IR}_c(t,\boldsymbol{k}) + a^3(t)\,V'(\phi^{\rm IR}_c)(t,\boldsymbol{k}) - \xi_\Pi(t,\boldsymbol{k})\,. \tag{A32b}$$

Consequently, we can perform the path integral $\int \mathcal{D}(\phi^{\rm IR}_\Delta, \Pi^{\rm IR}_\Delta)$, leading to

$$Z[J^{\rm IR}(T)] \simeq \prod_{k\le k_c(T)} \int {\rm d}\phi^{\rm IR}_c(T,\boldsymbol{k})\, e^{iJ^{\rm IR}\cdot\phi^{\rm IR}_c} \int \mathcal{D}(\xi_\phi,\xi_\Pi)\, P[\xi_\phi,\xi_\Pi]\Big|_{\mathcal{L}_\phi=\mathcal{L}_\Pi=0\ \&\ (\text{A25})}. \tag{A33}$$

Now, we regard auxiliary fields (ξ_ϕ, ξ_Π) as noise variables whose correlations are given by

$$\begin{aligned}\langle \xi_\alpha(t,\boldsymbol{k})\xi_\beta(t',\boldsymbol{k}')\rangle &:= \int \mathcal{D}(\xi_\phi,\xi_\Pi)\, P[\xi_\phi,\xi_\Pi]\, \xi_\alpha(t,\boldsymbol{k})\xi_\beta(t',\boldsymbol{k}') \\ &= \left[\frac{i\delta}{\delta X_\alpha(t,\boldsymbol{k})}\frac{i\delta}{\delta X_\beta(t',\boldsymbol{k}')}\right] e^{i\left(\Gamma^{k>0}_{\rm LO}+\Gamma_{k=0}+S^{\rm IR}_{H,(s)}\right)}\Big|_{\phi^{\rm IR}_\Delta=\Pi^{\rm IR}_\Delta=0},\end{aligned} \tag{A34}$$

where $\alpha,\beta = (\phi,\Pi)$ and $(X_\phi, X_\Pi) = (\Pi^{\rm IR}_\Delta, -\phi^{\rm IR}_\Delta)$ following the notation in (A14). We also have the corresponding expression in the momentum space. If we ignore $S_{H,(s)}$ and $i\Gamma_{k=0}$, we have

$$\langle \xi_\alpha(t,\boldsymbol{k})\xi_\beta(t',\boldsymbol{k}')\rangle = (2\pi)^3\delta(\boldsymbol{k}+\boldsymbol{k}')\,{\rm Re}\Big[g^{\alpha\beta}(t)\Big]\delta(t-t')\delta(t-t_k)\,. \tag{A35}$$

Equation (A33) shows that the effective dynamics of IR fields are described by the set of Langevin equations $\mathcal{L}_\phi = \mathcal{L}_\Pi = 0$ with the initial condition (A25) and the noise correlations (A35).

In the real space, the dynamics is described by the set of Langevin equations,

$$\dot\phi^{\rm IR}_c(x) = a^{-3}(t)\Pi^{\rm IR}_c(x) + \xi_\phi(x)\,, \tag{A36a}$$

$$\dot\Pi^{\rm IR}_c(x) = a(t)\nabla^2\phi^{\rm IR}_c(x) - a^3V'(\phi^{\rm IR}_c(x)) + \xi_\Pi(x)\,, \tag{A36b}$$

with the initial conditions (A26) and the noise correlations

$$\langle \xi_\alpha(x)\xi_\beta(y)\rangle = G^{\alpha\beta}(x,y)\,. \tag{A37}$$

Equation (A33) takes the following form in the real space:

$$Z[J^{\rm IR}(T)] \simeq \prod_{\boldsymbol{x}} \int {\rm d}\phi^{\rm IR}_c(T,\boldsymbol{x})\, e^{iJ^{\rm IR}\cdot\phi^{\rm IR}_c} \int \mathcal{D}(\xi_\phi,\xi_\Pi)\, P[\xi_\phi,\xi_\Pi]\Big|_{(\text{A26})\ \&\ (\text{A36})}. \tag{A38}$$

Substituting (A38) into (37), we have

$$\begin{aligned} p(\{\phi^{\rm IR}(T,\boldsymbol{x})\}_{T,\boldsymbol{x}\in\mathcal{D}}) \simeq \prod_{\boldsymbol{y}} \int {\rm d}\phi^{\rm IR}_c(T,\boldsymbol{y}) \prod_{\boldsymbol{x}\in\mathcal{D}} \delta(\phi^{\rm IR}_c(T,\boldsymbol{x}) - \phi^{\rm IR}(T,\boldsymbol{x})) \\ \times \int \mathcal{D}(\xi_\phi,\xi_\Pi)\, P[\xi_\phi,\xi_\Pi]\Big|_{(\text{A26})\ \&\ (\text{A36})}. \end{aligned} \tag{A39}$$

This expression provides a stochastic interpretation of the transition probability; the dynamics of $\phi^{\rm IR}_c$ are described by the set of Langevin equations, and the transition probability is simply understood as the probability to realize the field configuration $\phi^{\rm IR}_c(T,\boldsymbol{x}) = \phi^{\rm IR}(T,\boldsymbol{x})$ in the domain $\boldsymbol{x}\in\mathcal{D}$ at the final time T starting from the initial configuration $\phi^{\rm IR}_c(-\infty,\boldsymbol{x}) = \phi_{\rm false}$. In particular, the set of Langevin equations is given by (8) with the noise correlations (15) when we ignore the terms $\delta H_{\rm higher}$, $S^{\rm IR}_{H,(s)}$, and $\Gamma_{k=0}$. Note that such terms simply correct the Langevin equations[14] and do not invalidate the above stochastic interpretation.

Appendix B. Coleman–de Luccia Tunneling in Euclidean Method

In this appendix, we provide the CDL action in the de Sitter background with the Euclidean method.

Generally, the ways of Euclideanization for the de Sitter spacetime depend on the coordinates. In this paper, we discuss the field theory on the metric (1), and then we choose the following coordinate again[15].

$$\mathrm{d}s^2 = \frac{1}{H^2\eta^2}(-\mathrm{d}\eta^2 + \mathrm{d}\boldsymbol{x}^2). \tag{A40}$$

By taking the wick rotation as $\eta \to -i\tau$, the coordinate becomes

$$-\mathrm{d}s^2 = \frac{1}{H^2\tau^2}(\mathrm{d}\tau^2 + \mathrm{d}\boldsymbol{x}^2). \tag{A41}$$

This is the Euclidean AdS space discussed in Section 5, and we can take the global coordinate

$$-\mathrm{d}s^2 = H^{-2}(\mathrm{d}\rho^2 + \sinh^2\rho \mathrm{d}\Omega^2). \tag{A42}$$

We also impose that the field ϕ only depends on ρ. Therefore, the Euclidean action I^E and the equation of motion becomes

$$I^E = 2\pi^2 \int_0^\infty \mathrm{d}\rho \sinh^3\rho \left[\frac{1}{2H^2}(\partial_\rho\phi)^2 + \frac{V(\phi)}{H^4}\right], \tag{A43}$$

$$\frac{\mathrm{d}^2\phi}{\mathrm{d}\rho^2} + \frac{3}{\tanh\rho}\frac{\mathrm{d}\phi}{\mathrm{d}\rho} = \frac{V'(\phi)}{H^2}. \tag{A44}$$

The second equation is the same as (82), and we can obtain the same bounce solutions discussed in Section 5. For numerical calculations, we consider the potential (42) and fitting function (84). Also, we take the following non-dimensionalizations;

$$\phi = \alpha\tilde{\phi}, \tag{A45}$$

$$V(\phi) = g^2\alpha^4\tilde{V}(\tilde{\phi}). \tag{A46}$$

Therefore, the Euclidean action (A43) becomes

$$\begin{aligned} I^E &= 2\pi^2\frac{\alpha^2}{H^2}\int_0^\infty \mathrm{d}\rho \sinh^3\rho\left[\frac{1}{2}(\partial_\rho\tilde{\phi})^2 + \frac{g^2\alpha^2}{H^2}\tilde{V}(\tilde{\phi})\right] \\ &:= 2\pi^2\frac{\alpha^2}{H^2}\tilde{I}^E. \end{aligned} \tag{A47}$$

The ratio of the Coleman–de Luccia Euclidean action I^E_{bounce} to the Hawking–Moss action I_{HM} is given by

$$\gamma_E = \frac{I^E_{\mathrm{bounce}}}{I_{\mathrm{HM}}} = \frac{H^2}{g^2\alpha^2}\frac{9\tilde{I}^E_{\mathrm{bounce}}}{(1-\beta)^3(\beta+3)}. \tag{A48}$$

Notes

1 For earlier discussions of a stochastic approach based on the Schwinger–Keldysh formalism, see, e.g., [11,24].

2 Generally, we can choose other discretization like Stratonovich's discretization. This ambiguity does not affect the result since the amplitudes of the noise do not depend on fields within the range of our approximation.

3 Precisely, $\hat{\phi}^{\mathrm{IR}}(\boldsymbol{x})$ is defined in terms of the the Schrödinger picture field $\hat{\phi}(\boldsymbol{k})$ in momentum space as $\hat{\phi}^{\mathrm{IR}}(\boldsymbol{x}) := \int \frac{\mathrm{d}^3k}{(2\pi)^3}\hat{\phi}(\boldsymbol{k})\, e^{i\boldsymbol{k}.\boldsymbol{x}}\theta(k_c(t)-k)$. We have suppressed the trivial time dependence stemming from the step function.

4 There is a subtlety that modes satisfying $k \geq k_c(T)$ are initially regarded as the "UV" degrees of freedom (DoFs) while they become "IR" DoFs due to the accelerating expansion of the spacetime. However, by adopting this splitting procedure, we can use the Schwinger–Keldysh (or *closed-time-path*) formalism to evaluate the integration over UV variables first as usual.

5 This is consistent with the observation made in [6] that an HM solution corresponds to the transition over a region of a Hubble horizon volume.

[6] Note that this behavior may motivate one to replace the term $j_0(k_c(t)r)$ in (55) by the step function

$$j_0(k_c(t)r) \to \theta(1 - k_c(t)r)\,. \tag{A49}$$

This is the approximation adopted in [8].

[7] Note that we can also estimate the action I by performing the coarse-graining in time suitably and substituting the smeared expression of Π_Δ into the action:

$$I \simeq -\frac{8\pi^2}{3H^4}\int_{t'}^{t_*} \mathrm{d}t\, V'(\phi_c(t,\boldsymbol{x}_0)) \int \mathrm{d}^3x\, \dot{\phi}_c(t,\boldsymbol{x}) W_f(r;t) \simeq -\frac{8\pi^2}{3H^4}\int_{t'}^{t_*} \mathrm{d}t\, \dot{\phi}_c(t,\boldsymbol{x}_0) V'(\phi_c(t,\boldsymbol{x}_0)) = -\frac{8\pi^2}{3H^4}\Delta V\,,$$

reproducing the previous result (52). In the first approximate equality, we used $H_{\mathrm{HM}} = 0$, which is well satisfied after the smearing. In the second one, we used $\phi_c(t,\boldsymbol{x}) \simeq \phi_c(t,\boldsymbol{x}_0)$ for $r \ll k_c^{-1}(t)$ and the condition $\int \mathrm{d}^3x\, W_f(r;t) = 1$ which follows from the definition of W_f. This estimate may be more analogous to the calculation of the action in Section 4.1 since the approximate locality of the dynamics is restored after the smearing.

[8] This is the reason why we illustrate flow lines in the (ϕ_c, ϕ_Δ)-plane in Figure 5.

[9] This is compatible with the condition $\varepsilon < \alpha/H$ when the weak coupling $g \ll 1$ is considered.

[10] We can also compare δH with the second and the third term on the RHS of (73). Such considerations do not change our estimate of $\varepsilon_{\max}$ in (88).

[11] In the main text, we use the notation $X_{\boldsymbol{k}}(t)$ to write variables in momentum space. However, we adopt the notation $X(t,\boldsymbol{k})$ in this appendix since we have many subscripts such as c and Δ.

[12] Here, 0^+ is the infinitesimal time step which is introduced to obtain the path integral representation of the unitary time evolution as usual.

[13] Precisely speaking, we need to perform the UV–IR splitting in the path integral with an infinitesimal discrete time step for deriving S_{tr} correctly. After taking the continuum limit, we obtain (A8); see also [23]. Furthermore, the form of $S_{\text{mix-int}}$ depends on the model. In our case, we have

$$\begin{aligned} S_{\text{mix-int}} = \int \mathrm{d}^4x \big[& V(\phi_+^{\mathrm{UV}} + \phi_+^{\mathrm{IR}}) - V(\phi_+^{\mathrm{UV}}) - V(\phi_+^{\mathrm{IR}}) \\ & - V(\phi_-^{\mathrm{UV}} + \phi_-^{\mathrm{IR}}) + V(\phi_-^{\mathrm{UV}}) + V(\phi_-^{\mathrm{IR}}) \big]_{\phi_\pm^{\mathrm{UV}} = \phi_c^{\mathrm{UV}} \pm (\phi_\Delta^{\mathrm{UV}}/2),\, \phi_\pm^{\mathrm{IR}} = \phi_c^{\mathrm{IR}} \pm (\phi_\Delta^{\mathrm{IR}}/2)}\,. \end{aligned} \tag{A50}$$

[14] For instance, leading-order corrections to the stochastic dynamics at the super-horizon scales are calculated in [22].

[15] The analytic continuation of this coordinate is examined in [5].

References

1. Coleman, S.R. The Fate of the False Vacuum. 1. Semiclassical Theory. *Phys. Rev. D* **1977**, *15*, 2929–2936; Erratum in *Phys. Rev. D* **1977**, *16*, 1248. [CrossRef]
2. Callan, C.G., Jr.; Coleman, S.R. The Fate of the False Vacuum. 2. First Quantum Corrections. *Phys. Rev. D* **1977**, *16*, 1762–1768. [CrossRef]
3. Coleman, S.R.; De Luccia, F. Gravitational Effects on and of Vacuum Decay. *Phys. Rev. D* **1980**, *21*, 3305. [CrossRef]
4. Hawking, S.W.; Moss, I.G. Supercooled Phase Transitions in the Very Early Universe. *Phys. Lett. B* **1982**, *110*, 35–38. [CrossRef]
5. Rubakov, V.A.; Sibiryakov, S.M. False vacuum decay in de Sitter space-time. *Theor. Math. Phys.* **1999**, *120*, 1194–1212. [CrossRef]
6. Brown, A.R.; Weinberg, E.J. Thermal derivation of the Coleman-De Luccia tunneling prescription. *Phys. Rev. D* **2007**, *76*, 064003. [CrossRef]
7. Starobinsky, A.A. Stochastic de Sitter (Inflationary) Stage in the Early Universe. *Lect. Notes Phys.* **1986**, *246*, 107–126. [CrossRef]
8. Starobinsky, A.A.; Yokoyama, J. Equilibrium state of a selfinteracting scalar field in the De Sitter background. *Phys. Rev. D* **1994**, *50*, 6357–6368. [CrossRef] [PubMed]
9. Goncharov, A.S.; Linde, A.D.; Mukhanov, V.F. The Global Structure of the Inflationary Universe. *Int. J. Mod. Phys. A* **1987**, *2*, 561–591. [CrossRef]
10. Linde, A.D. Hard art of the universe creation (stochastic approach to tunneling and baby universe formation). *Nucl. Phys. B* **1992**, *372*, 421–442. [CrossRef]
11. Tolley, A.J.; Wyman, M. Stochastic tunneling in DBI inflation. *J. Cosmol. Astropart. Phys.* **2009**, *10*, 006. [CrossRef]
12. Noorbala, M.; Vennin, V.; Assadullahi, H.; Firouzjahi, H.; Wands, D. Tunneling in Stochastic Inflation. *J. Cosmol. Astropart. Phys.* **2018**, *09*, 032. [CrossRef]
13. Hashiba, S.; Yamada, Y.; Yokoyama, J. Particle production induced by vacuum decay in real time dynamics. *Phys. Rev. D* **2021**, *103*, 045006. [CrossRef]
14. Camargo-Molina, J.E.; Rajantie, A. Phase transitions in de Sitter: The stochastic formalism. *arXiv* **2022**, arXiv:2204.02875.

15. Camargo-Molina, J.E.; González, M.C.; Rajantie, A. Phase Transitions in de Sitter: Quantum Corrections *arXiv* **2022**, arXiv:2204.03480.
16. Martin, P.C.; Siggia, E.D.; Rose, H.A. Statistical Dynamics of Classical Systems. *Phys. Rev. A* **1973**, *8*, 423–437. [CrossRef]
17. De Dominicis, C.; Brezin, E.; Zinn-Justin, J. Field Theoretic Techniques and Critical Dynamics. 1. Ginzburg-Landau Stochastic Models Without Energy Conservation. *Phys. Rev. B* **1975**, *12*, 4945. [CrossRef]
18. Janssen, H.K. On a Lagrangean for classical field dynamics and renormalization group calculations of dynamical critical properties. *Z. Phys. B Condens. Matter* **1976**, *23*, 377–380. [CrossRef]
19. De Dominicis, C.; Peliti, L. Field Theory Renormalization and Critical Dynamics Above t(c): Helium, Antiferromagnets and Liquid Gas Systems. *Phys. Rev. B* **1978**, *18*, 353–376. [CrossRef]
20. Elgart, V.; Kamenev, A. Rare event statistics in reaction-diffusion systems. *Phys. Rev. E* **2004**, *70*, 041106. [CrossRef]
21. Altland, A.; Simons, B.D. *Condensed Matter Field Theory*, 2nd ed.; Cambridge University Press: Cambridge, UK, 2010. [CrossRef]
22. Tokuda, J.; Tanaka, T. Statistical nature of infrared dynamics on de Sitter background. *J. Cosmol. Astropart. Phys.* **2018**, *02*, 014. [CrossRef]
23. Tokuda, J.; Tanaka, T. Can all the infrared secular growth really be understood as increase of classical statistical variance? *J. Cosmol. Astropart. Phys.* **2018**, *11*, 022. [CrossRef]
24. Morikawa, M. Dissipation and Fluctuation of Quantum Fields in Expanding Universes. *Phys. Rev. D* **1990**, *42*, 1027–1034. [CrossRef] [PubMed]
25. Feynman, R.P.; Vernon, F.L., Jr. The Theory of a general quantum system interacting with a linear dissipative system. *Ann. Phys.* **1963**, *24*, 118–173. [CrossRef]
26. Weinberg, E.J. *Classical Solutions in Quantum Field Theory: Solitons and Instantons in High Energy Physics*; Cambridge Monographs on Mathematical Physics, Cambridge University Press: Cambridge, UK, 2012. [CrossRef]
27. Weinberg, E.J. Hawking-Moss bounces and vacuum decay rates. *Phys. Rev. Lett.* **2007**, *98*, 251303. [CrossRef] [PubMed]
28. Jensen, L.G.; Steinhardt, P.J. Bubble Nucleation and the Coleman-Weinberg Model. *Nucl. Phys. B* **1984**, *237*, 176–188. [CrossRef]
29. Jensen, L.G.; Steinhardt, P.J. Bubble Nucleation for Flat Potential Barriers. *Nucl. Phys. B* **1989**, *317*, 693–705. [CrossRef]
30. Hackworth, J.C.; Weinberg, E.J. Oscillating bounce solutions and vacuum tunneling in de Sitter spacetime. *Phys. Rev. D* **2005**, *71*, 044014. [CrossRef]
31. Batra, P.; Kleban, M. Transitions Between de Sitter Minima. *Phys. Rev. D* **2007**, *76*, 103510. [CrossRef]
32. Braden, J.; Johnson, M.C.; Peiris, H.V.; Pontzen, A.; Weinfurtner, S. New Semiclassical Picture of Vacuum Decay. *Phys. Rev. Lett.* **2019**, *123*, 031601; Erratum in *Phys. Rev. Lett.* **2022**, *129*, 059901. [CrossRef]
33. Blanco-Pillado, J.J.; Deng, H.; Vilenkin, A. Flyover vacuum decay. *J. Cosmol. Astropart. Phys.* **2019**, *12*, 001. [CrossRef]
34. Hertzberg, M.P.; Rompineve, F.; Shah, N. Quantitative Analysis of the Stochastic Approach to Quantum Tunneling. *Phys. Rev. D* **2020**, *102*, 076003. [CrossRef]
35. Tranberg, A.; Ungersbäck, G. Bubble nucleation and quantum initial conditions in classical statistical simulations. *J. High Energy Phys.* **2022**, *09*, 206. [CrossRef]
36. Hertzberg, M.P.; Yamada, M. Vacuum Decay in Real Time and Imaginary Time Formalisms. *Phys. Rev. D* **2019**, *100*, 016011. [CrossRef]
37. Kristiano, J.; Lambaga, R.D.; Ramadhan, H.S. Coleman-de Luccia Tunneling Wave Function. *Phys. Lett. B* **2019**, *796*, 225–229. [CrossRef]
38. Cespedes, S.; de Alwis, S.P.; Muia, F.; Quevedo, F. Lorentzian vacuum transitions: Open or closed universes? *Phys. Rev. D* **2021**, *104*, 026013. [CrossRef]
39. Maniccia, G.; De Angelis, M.; Montani, G. WKB Approaches to Restore Time in Quantum Cosmology: Predictions and Shortcomings. *Universe* **2022**, *8*, 556. [CrossRef]
40. Espinosa, J.R. Fresh look at the calculation of tunneling actions including gravitational effects. *Phys. Rev. D* **2019**, *100*, 104007. [CrossRef]
41. Gregory, R.; Moss, I.G.; Oshita, N. Black Holes, Oscillating Instantons, and the Hawking-Moss transition. *J. High Energy Phys.* **2020**, *07*, 024. [CrossRef]
42. Gregory, R.; Moss, I.G.; Oshita, N.; Patrick, S. Hawking-Moss transition with a black hole seed. *J. High Energy Phys.* **2020**, *09*, 135. [CrossRef]
43. Freese, K.; Spolyar, D. Chain inflation: 'Bubble bubble toil and trouble'. *J. Cosmol. Astropart. Phys.* **2005**, *07*, 007. [CrossRef]
44. Berera, A. Warm inflation. *Phys. Rev. Lett.* **1995**, *75*, 3218–3221. [CrossRef] [PubMed]